scientific reports

Check for updates

OPEN

Improved security for IoT-based remote healthcare systems using deep learning with jellyfish search optimization algorithm

Faris Kateb[1], Mahmoud Ragab[1,2]✉, Felwa Abukhodair[1,2], Omar Ahmed Abdulkader[3], Louai A. Maghrabi[4], Sami Saeed Binyamin[5] & Mohammed Khaled Al-Hanawi[6]

With an increased chronic disease and an ageing population, remote health monitoring is a substantial method to enhance the care of patients and decrease healthcare expenses. The Internet of Things (IoT) presents a promising solution for remote health monitoring by collecting and analyzing vital data like body temperature, ECG, and heart rate, giving real-time insights to medical professionals. However, maintaining effectual monitoring in environments with bandwidth or energy constraints presents crucial threats. While machine analysis and human insight performance must be content, conveying extra data to gratify both would be evaded for efficient resource application. Therefore, this article proposes an Enhanced Security Mechanism for Human-Centered Systems using Deep Learning with Jellyfish Search Optimizer (ESHCS-DLJSO) approach for IoT healthcare applications. The projected ESHCS-DLJSO approach allows IoT devices in the healthcare field to securely convey medical data and early recognition of health problems in the human-machine interface. To achieve this, the ESHCS-DLJSO approach utilizes a min-max normalization technique to transform the input data into a more suitable format. The bacterial foraging optimization algorithm (BFOA) method is used for feature extraction. Moreover, a convolutional neural network with long short-term memory (CNN-LSTM-Attention) technique is used for disease detection and classification. Finally, the ESHCS-DLJSO technique employs the jellyfish search optimizer (JSO) technique for hyperparameter tuning. The simulation of the ESHCS-DLJSO technique is examined on an IoT healthcare security dataset. The performance validation of the ESHCS-DLJSO technique portrayed a superior accuracy value of 99.43% over existing approaches.

Keywords Internet of things, Deep learning, Jellyfish search optimizer, Human-centered systems, Healthcare, Bacterial foraging optimization algorithm

Humans are still looking for more normal sensing and manual feature developments. Such developments can be related to some cognition transformation generated by human intuition to be modified to novel variations in living standards[1]. Owing to the differential progress in the difficulty of mechanical frameworks and the resulting need for communication among the machine functionalities and human perceptions, human-machine interfaces (HMIs) come into existence; HMI structures can significantly help humans using a large number of physical abilities and ages to use and controlling machinery[2]. Figure 1 represents the structure of Human-Centered systems. Using fast growth in the IoT in the last few years, HMIs have progressively been developed. It is a beneficial technology for providing innovative remote healthcare, including IoT-authorised devices by medical appliances[3]. Incorporating IoT and deep learning (DL) techniques has transformed healthcare processes in domestic areas by supporting remote health supervision and initial identification of health-related problems. The IoT technology application allows the collection of vast amounts of physiological information, namely body

[1]Information Technology Department, Faculty of Computing and Information Technology, King Abdulaziz University, Jeddah 21589, Saudi Arabia. [2]Center of Excellence in Smart Environment Research, King Abdulaziz University, Jeddah21589, Saudi Arabia. [3]Faculty of Computer Studies, Arab Open University, Riyadh, Saudi Arabia. [4]Department of Software Engineering, College of Engineering, University of Business and Technology, Jeddah, Saudi Arabia. [5]Computer and Information Technology Department, The Applied College, King Abdulaziz University, Jeddah 21589, Saudi Arabia. [6]Health Services and Hospitals Administration Department, Faculty of Economics and Administration, King Abdulaziz University, Jeddah 21589, Saudi Arabia. ✉email: mragab@kau.edu.sa

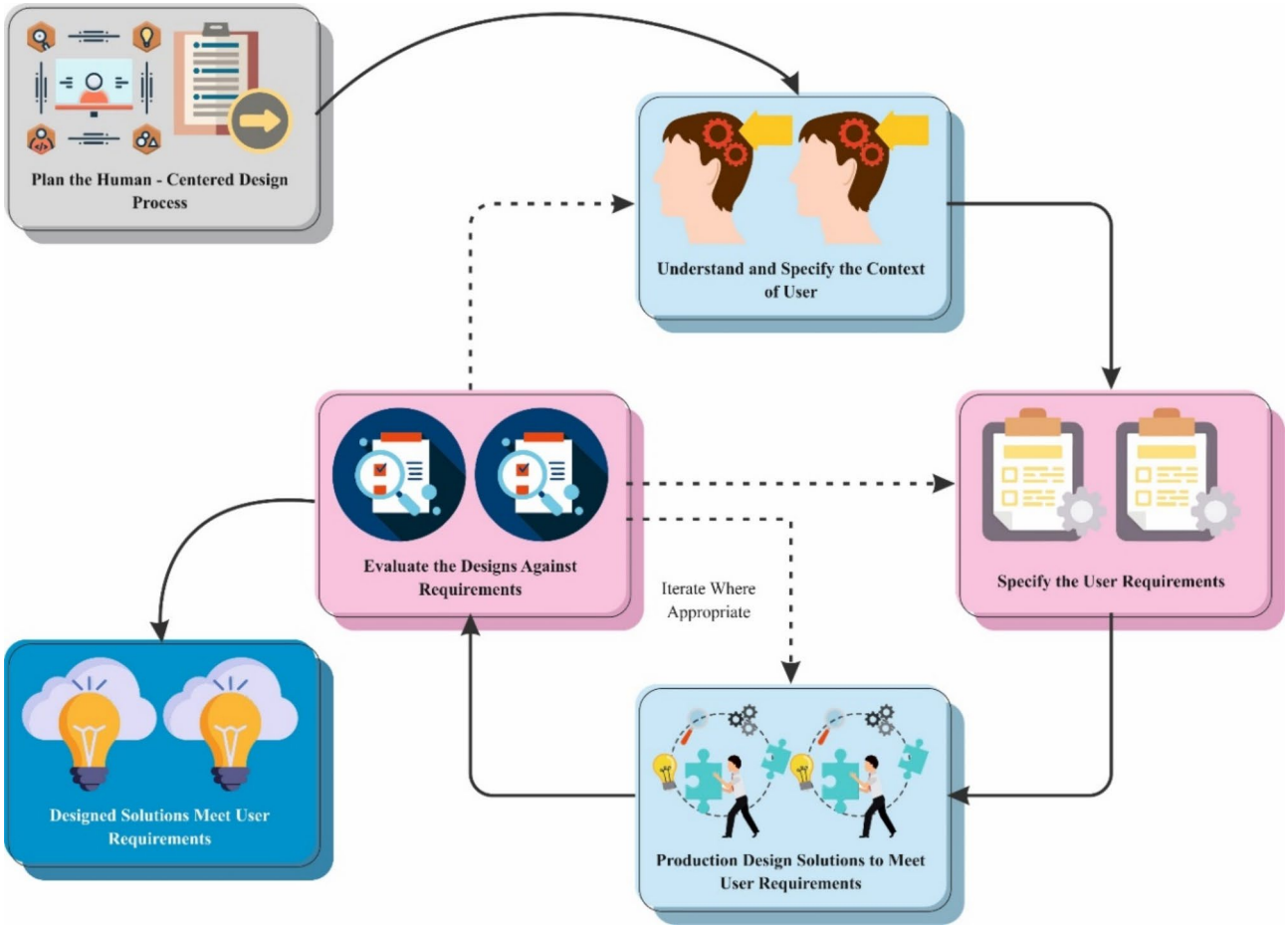

Fig. 1. Structure of human-centered systems.

temperature, blood oxygen level, ECG signals, and heart rate, from appropriate sensors or devices[4]. IoT offers instant admission to doctors and hospitals by calculating and treating a fundamental symptom of patients. These help to reduce the mortality rate produced because of heart failures and strokes. IoT implementation techniques continually change people's day-to-day life approaches[5]. IoT technologies will additionally improve human culture into an innovative period of human-machine combination, collaborative sharing and design, and intelligence. DL methods and IoT technologies are broadly applied in many arenas to support the technological foundations of the recent technological revolt. Many machine learning (ML) techniques have been used in decision-making in healthcare appliances[6].

Nevertheless, many traditional approaches like classic neural networks and k-nearest neighbours are only suitable if the data scale rises in time and vast quantities of data as big data have been made. On the other hand, DL models are hopeful substitutions in this connection, with tactics in deep architectures for learning hierarchical depictions[7]. These approaches can handle significant quantities of data, but the precision increases with the growth of training data sets. Convolutional neural networks (CNN) are the best model for DL approaches that are effective for IoT-based medical observation. CNN is a deep NN class frequently applied with 2D signs, namely images and videos. They might have been learning thousands of objects with millions of images as input data sets. Attention layers allow the DL methods to concentrate on particular input data features that are more related to the classification task[8]. These increase precision and reduce computational efficiency, making it appropriate for placement in limited resource environments like home health care services. The swift evolution of IoT technologies has significantly improved the potential for remote healthcare systems, but confirming robust security remains a critical threat. With the growing dependence on connected devices to monitor and manage human health, safeguarding sensitive data and ensuring the integrity of health data is essential[9]. As healthcare systems become more intrinsic and data-driven, there is a growing requirement for enhanced security mechanisms that can adapt to the dynamic nature of IoT environments. Employing DL and optimization models presents a promising approach to improving the security and effectualness of these systems. By incorporating intelligent models with IoT infrastructure, it is possible to build more resilient and responsive healthcare solutions prioritizing privacy and functionality[10].

This article proposes an Enhanced Security Mechanism on Human-Centered Systems using DL with Jellyfish Search Optimizer (ESHCS-DLJSO) approach for IoT healthcare applications. The projected ESHCS-DLJSO approach allows IoT devices in the healthcare field to securely convey medical data and early recognition of

health problems in the human-machine interface. To achieve this, the ESHCS-DLJSO approach utilizes a min-max normalization technique to transform the input data into a more suitable format. The bacterial foraging optimization algorithm (BFOA) method is used for feature extraction. Moreover, a convolutional neural network with long short-term memory (CNN-LSTM-Attention) technique is used for disease detection and classification. Finally, the ESHCS-DLJSO technique employs the jellyfish search optimizer (JSO) technique for hyperparameter tuning. The simulation of the ESHCS-DLJSO technique is examined on an IoT healthcare security dataset. The major contribution of the ESHCS-DLJSO technique is listed below.

- The ESHCS-DLJSO model utilizes Min-max normalization to scale and standardize the input data, confirming consistent value ranges. This pre-processing step improves the technique's capability to learn and generalize more effectively. Converting the data into an appropriate format enhances the overall effectiveness of subsequent analyses and models.
- The BFOA approach detects and extracts the most relevant features from the data. This methodology optimizes the feature selection process, enhancing the model's accuracy and reducing computational complexity. Concentrating on key features improves the efficiency of disease detection and classification.
- The CNN-LSTM-Attention model is employed for precise disease detection and classification, incorporating the merits of convolutional and recurrent networks. This hybrid methodology captures spatial and temporal patterns in the data, enhancing classification accuracy. The attention mechanism improves the method's focus on the most relevant features, confirming robust performance.
- The JSO method is implemented to fine-tune the model parameters, enhancing their accuracy and effectiveness. This optimization methodology intelligently alters the parameters to attain optimal performance. By improving the model's adaptability, JSO confirms enhanced generalization and faster convergence during training.
- Integrating advanced optimization approaches such as JSO with DL models—CNN-LSTM-Attention presents a novel solution for disease classification in IoT-based healthcare systems—and improves the classification process's accuracy and efficiency. The ability to fine-tune models dynamically while capturing complex patterns in data represents a crucial enhancement in healthcare diagnostics.

The article is structured as follows: "Literature survey" presents the literature review, "Proposed method" outlines the proposed method, "Result analysis" details the results evaluation, and "Conclusion" concludes the study.

Literature survey

Mohapatra et al.[11] presented a time-frequency domain deep neural network (TFDDNN)-based method for recognizing hand signals with MEMG footage. The MEMG footage has been segmented within frames, and the average of each channel data (mean EMG signal) to all frames is estimated. The constant wavelet transformation can be used in the mean EMG signal to obtain the combined time-frequency representation (TFR). The TFR-based imageries of the mean EMG signal are employed as input into the deep representation learning network (DRLN) method for recognizing hand signals. Wang et al.[12] introduced an HMI-obtained image coding (HMI-IC) outline depending on DL. In these models, machinery must offer initial supervising messages containing study outcomes and sample images; humans can also request first-class imageries of key elements. Adaptive coding transmission can be adequate for various needs in two phases based on a lack of resources. Islam et al.[13] developed an IoT-based method for isolated supervision and earlier identification of health difficulties in-home medical backgrounds. The data collected will be transferred to the server using the MQTT protocol. The pre-trained DL method depends on a CNN by an attention layer utilized by the server for classifying possible illnesses. Rani et al.[14] designed a 3-phase product-economy-ecology approach by considering additive manufacturing techniques' fundamental functional and characteristic development. Key supporting techniques for product growth and process design have been conferred. Moreover, the usual implementations of human-machine collaborative additive manufacturing within the product, economic, and ecological phases were deliberated, containing modified product design, energy conservation, emission reduction, collaboration design, communicating manufacturing, distributed manufacturing, and HMI technologies for the process chain. In[15], an intense and intellectual IoMT process has been developed using the synergistic incorporation of flexible wearable triboelectric sensors and DL-helped data analytics. This approach embedded four triboelectric sensors within a wristband for detecting and analyzing limb movements in patients struggling with Parkinson's Disease (PD). Webber et al.[16] introduced a method for identifying signals in handling intermittent light patterns in a visible light communications (VLC) approach. This process achieves the current light communications framework with cheaper and freely obtainable mechanisms. Various finger orders have been recognized with probabilistic neural networks (PNNs) trained on light transitions among fingers. The unique pre-processing from the tested light on a photodiode is defined to assist the usage of the PNN by deficient intricateness. Shoukat et al.[17] recommend implementing the DT method and summarising the study and application growth from the view of the home devices' DT modelling. The modelling technique was three-phase: regarding a virtual entity, physical entity, and data communication connectivity. The presented approach uses communication methods for the intellectual control of HD by incorporating DT and virtual simulation technology to establish a human CPS, primarily directing tasks related to remote-control difficulties.

Nguyen et al.[18] developed a wrist-worn prototype for capturing an RGB video for a hand signals stream. This approach then estimates different CNN techniques for vision-based detection. Moreover, this approach analyzes the method that provides the finest trade-off amongst memory requirement, cost of computation, and accuracy. This approach demonstrates that when analyzing architecture, MoviNet gives the maximum precision. At that time, a unique MoviNet-based 2-stream architecture was presented, which takes either RGB or optical flow within the version. Vakili et al.[19] present a service composition methodology using Grey Wolf Optimization

(GWO) and MapReduce framework to compose services with optimized QoS. Heidari et al.[20] propose a blockchain (BC)-based federated learning (FL) method to confirm data privacy, utilizing SegCaps, CNN, and transfer learning (TL) for enhanced image feature extraction and model performance. Pavithra et al.[21] introduce an Optimized Deep Recurrent Neural Network (O-DRNN) method with a secure multitier architecture, utilizing PSO for feature selection and Bayesian optimization for hyperparameter tuning, with edge computing and cloud storage secured by ECKAS. Aminizadeh et al.[22] comprehensively review ML, DL, and distributed systems in healthcare to improve service quality and address key implementation threats. Amiri et al.[23] review and synthesize DL applications in IoT-based bio- and medical informatics, classifying them by technique to address medical threats. Kumar et al.[24] introduce a DL-based DL approach for secure data transmission (BDSDT) in IoT healthcare by utilizing ZKP for integrity, IPFS for storage, and Ethereum smart contracts for security, with DSAE-BiLSTM for intrusion detection. Heidari et al.[25] propose an approach that constructs an optimal spanning tree by incorporating artificial bee colony (ABC), genetic operators, and density correlation to optimize device connectivity by depending on hop count, residual energy, and mobility. Heidari, Navimipour, and Unal[26] present a DL-based RBFNN methodology to enhance data integrity and storage for smart decision-making in IoDs. Heidari et al.[27] analyze the availability and reliability of Wireless Sensor Networks (WSNs) by examining failure scenarios utilizing fault trees and Markov chain analysis to enhance network stability. Singh et al.[28] introduce a continuous authentication system for IoT healthcare using LSTM, integrating biometric data and security credentials to prevent unauthorized access, with data collected via Arduino Uno and smart devices. Zanbouri et al.[29] propose a GSO-based optimization model for DL-based IIoT, enhancing scalability, resource allocation, and decision-making to mitigate inefficiencies and bottlenecks. Amiri, Heidari, and Navimipour[30] introduce a novel taxonomy for DL applications in climate change mitigation. It classifies ML methods into six key areas and underscores advanced research.

Rajkumar et al.[31] employ the DL model for heart disease prediction, pre-processing data with Median Studentized Residual, selecting features with Harris Hawk Optimization (HHO), and classifying with Modified Deep LSTM, optimized by Improved Spotted Hyena Optimization (ISHO). Aldaej, Ahanger, and Ullah[32] present a secure IoT healthcare diagnostic model by employing deep neural networks (DNNs), integrating encryption, safe transactions, and techniques like orthogonal particle swarm optimization (PSO) for medical image sharing and neighbourhood indexing for hash value encryption. Movassagh et al.[33] focus on improving perceptron neural network precision by utilizing meta-heuristic algorithms for training and determining input coefficients. Babar et al.[34] develop a secure, intelligent, and efficient framework for smart H-CIoT networks using Software-Defined Networking (SDN) and DL, addressing challenges like attack detection, data management, and fog node selection. Kumar et al.[35] propose a virtual object management system utilizing Digital Twins (DT) for optimal task scheduling and enhanced user experience. It employs Hybrid Energy Valley with Lévy Flight Distribution Optimization (HEV-LFDO) for efficient task offloading to edge devices while securing data with BC for effective resource management and minimizing local loss. Othmen et al.[36] optimize cluster head (CH) selection and routing paths in IoT-enabled healthcare applications utilizing fuzzy logic (FL) and PSO to improve communication efficiency, reduce delays, and enhance throughput and energy efficiency. Alzubi[37] presents a BC-based secure system for medical IoT devices using Lamport Merkle Digital Signature (LMDS). It authenticates devices through a tree structure of patient data hashes, with a Centralized Healthcare Controller verifying the root using LMDS Verification. Rani et al.[38] developed an IoT-based healthcare system using SqueezeNet_Fractional Dung Beetle Optimization (SqueezeNet_FDBO), optimizing routing and classification performance. Alzubi et al.[39] introduce a technique incorporating DL and BC for electronic health record privacy. Using a CNN classifies users as normal or abnormal, then removes abnormal users via BC and cryptography-based FL, securing access to health records. Radhika et al.[40] developed a Binary Butterfly Optimization Algorithm with Stacked Non-symmetric Deep Auto-Encoder (BBOA-SNDAE) methodology for predicting HD using clinical data and Medical IoT technology. Naz et al.[41] developed a medical diagnostic system using IoT and CNN to precisely detect tumours, improving breast cancer diagnosis and early detection. While identifying future research opportunities, Bai, Gu, and Tang[42] explore how DL and IoT technologies can improve patient monitoring, clinical outcomes, and ICU processes. Table 1 summarizes the existing studies on remote healthcare.

The existing studies present various models for addressing key threats in IoT-based healthcare systems, comprising secure data transmission, disease prediction, and system optimization. Some approaches employ DL methods, such as LSTM, for continuous authentication and heart disease prediction, while others incorporate DL for improved data integrity and privacy in decentralized systems. HHO, Bayesian optimization, and PSO enhance feature selection and model performance. Several methodologies integrate IoT sensors for real-time data collection, optimizing resource allocation, and addressing issues such as scalability, security, and fault tolerance in healthcare networks. However, these methods mostly encounter limitations such as high computational complexity, scalability threats in dynamic environments, and potential data privacy and accuracy issues, which could affect their practical implementation and widespread adoption in real-world healthcare settings. The research gap is in the limited exploration of scalable, real-time DL and DL-based solutions for safe, effectual IoT healthcare systems, specifically in handling dynamic data and resource constraints. Furthermore, more comprehensive studies need to be conducted to address the incorporation of diverse optimization models and their real-world applicability in diverse healthcare environments.

Proposed method

This study presents an ESHCS-DLJSO technique for IoT healthcare applications. The technique's main intention is to permit IoT devices in the healthcare field to transform medical data and early recognize health issues in HMI. It contains four distinct processes: data normalization, BFOA-based feature selection, CNN-LSTM-Attention using the disease detection process, and JSO-based parameter selection. Figure 2 demonstrates the entire process of the ESHCS-DLJSO model.

References	Techniques	Metrics	Findings
11	TFDDNN, Continuous Wavelet Transform, DRLN, Multichannel Electromyogram Sensor Data	Accuracy	The TFDDNN-based method achieved accuracy rates of 92.73% and 80.33% for multiclass hand gesture recognition using MEMG data from two databases
12	Human-Machine Interaction-Oriented Image Coding, DL, Adaptive Coding Transmission, Layered Data Stream Compression, Two-Stage Adaptive Transmission	Accuracy, Inference Speed, Coding Efficiency	The proposed method enhances accuracy and inference speed for compressed images, with coding efficiency comparable to JPEG2000 in energy- and bandwidth-constrained visual monitoring scenarios
13	IoT-based System, MAX30100 Sensor, AD8232 ECG Sensor Module, MLX90614 Non-Contact Infrared Sensor, MQTT Protocol, Pre-trained DL model	Precision, Recall, F1-Score	The system efficiently detects heartbeats and classifies body temperature, giving real-time disease detection and automatic doctor alerts for critical abnormalities
14	Human-Cyber-Physical System, Human-Machine Collaborative Additive Manufacturing, IoTs, Artificial Intelligence, DT Technology, Extended Reality, Intelligent Materials	Product, Economy, Ecology model (3-level framework)	The framework adopts human-machine collaboration in Industry 5.0 additive manufacturing, enhancing product personalization and sustainability and integrating AI and IoT
15	Triboelectric sensors for flexible, wearable sensing, DL-assisted data analytics, Integration of sensor data with intelligent healthcare monitoring system	Location/trajectory tracking, Heart rate monitoring, Identity recognition, Motion and fine motor analysis	The system effectually captures subtle limb movements, giving precise health monitoring, cost-efficiency, and high sensitivity
16	PNN, VLC system, Light transitions	Accuracy, Impact of matrix size, and Gaussian spread function on accuracy	The system shows the potential for gesture recognition utilizing VLC technology, attaining 73% accuracy and exhibiting promise for incorporating with growing Li-Fi standards
17	DT, Human-Cyber-Physical System, Game theory, Virtual simulation technologies, Remote intelligent control and data communication	Equipment tracking test, Connectivity depth and range for home-device networks	The study highlights the feasibility of utilizing a DT model incorporated with HCPS for smart home devices, attaining effectual synchronization and positional accuracy in real-time remote-control applications
18	Wrist-worn prototype, CNNs, MoviNet-based two-stream architecture	Top-1 accuracy improvement, Evaluation of models based on accuracy, memory requirement, and computational cost	The MoviNet-based architecture improves gesture recognition accuracy while optimizing memory and computational cost, giving valuable insights for wrist-worn human-machine interaction
19	GWO, MapReduce framework, Service composition for IoT and cloud integration	Cost, Availability, Response time, Energy savings	The proposed model enhances energy savings by 40%, reduces response time by 14%, increases availability by 11%, and lowers cost by 24% compared to baseline approaches
20	BC-based FL, SegCaps for image feature extraction, CNNs, Capsule Networks, Data normalization technique, TL	Accuracy, Area Under the Curve	The proposed method enhances detection accuracy by 6.6% and improves AUC by 5.1%, outperforming six benchmark models and showing its efficiency in deepfake detection
21	O-DRNN, Multitier secured architecture, Elliptic Curve Key Agreement Scheme, PSO, Bayesian Optimization, Edge computing and cloud computing integration	Accuracy, Encryption latency	The proposed system attains enhanced accuracy and reduced encryption latency, portraying an enhanced performance in real-time health data collection and analysis with improved security in edge computing environments
22	ML, DL, CNNs, Long Short-Term Memory, Distributed Systems, IoTs	Quality of Service, Accuracy	The study underscores the impact of ML, DL, and dispersed systems in enhancing healthcare, specifically cardiovascular disease diagnosis and improving service accuracy
23	CNNs, RNNs, Generative Adversarial Networks, Multilayer Perceptron, Hybrid Methods	Accuracy, Precision, Recall, F1-Score, Latency, Adaptability, Scalability	The review underscores advanced DL models in medical informatics, focusing on their impact on diagnostics and treatment and addressing implementation threats
24	BC, Off-Chain Storage, Smart Contract, DL	Accuracy, Precision, Recall, F1-Score	The BDSDT model gives secure data transmission and accurate intrusion detection in IoT healthcare systems, attaining nearly 99% accuracy
25	ABC, Genetic operators, Density correlation degree, Spanning tree construction	Hop count distance, Residual energy, Mobility probabilities, Reliability, Energy consumption, Displacement probability	The proposed model improves data collection reliability in IIoT by optimizing spanning tree construction, surpassing conventional techniques in reliability, energy efficiency, and mobility
26	BC, Radial Basis Function Neural Networks, DL, IoT	Specificity, F1-score, Recall, Precision, Accuracy	The BC-based RBFNN model improves intrusion detection and data integrity in IoD networks
27	Fault trees analysis, Markov chain analysis	Network availability, Network reliability, Fault tolerance	The evaluation methods enhance WSN fault tolerance and reliability, enabling developers to make informed decisions to improve system performance
28	Long Short-Term Memory, Continuous authentication using biometric data, multi-factor authentication, Arduino Uno and smart devices	Accuracy, Precision, Recall, Specificity, F1-score	The LSTM-based system boosts IoT healthcare security by precisely detecting users and enabling real-time threat detection
29	BC, Glowworm Swarm Optimization	Throughput, Scalability, Efficiency, Performance, Security	The GSO-optimized BC approach significantly enhances IIoT system performance, scalability, and security related to traditional methods
30	ML, DL, CNNs	Accuracy, Scalability, Interpretability, Latency, Adaptability	CNNs dominate climate change mitigation studies, with Python as the main tool and classification tasks concentrating on accuracy, scalability, and interpretability
31	IoT, Median Studentized Residual Approach, HHO, Modified Deep Long Short-Term Memory, ISHO	Accuracy, Specificity, Sensitivity, F-Score, Kappa Value, Balanced Error Rate, Execution Time	The proposed approach attains 98.01% accuracy in heart disease prediction, outperforming existing models with reduced error rates
32	BC, DNNs, Orthogonal PSO, Neighborhood Indexing Sequence Method, Optimized DNN	F-Measure, Sensitivity, Specificity, Accuracy	The IoT healthcare model improves performance with an F-Measure of 96.25% and an accuracy of 93.26% while enhancing security using BC and optimized DL techniques
33	Integrated Algorithm	Coefficient Convergence, Prediction Error	The proposed algorithm showed better convergence and reduced prediction error than existing algorithms

Continued

References	Techniques	Metrics	Findings
[34]	SDN, DL, BiLSTM, CNN	Accuracy, F1-Score, Latency, Energy Consumption, Probability	The proposed framework outperforms existing methods with higher accuracy, F1-score, lower latency, energy consumption, and improved probability
[35]	Hybrid Energy Valley, HEV-LFDO, BC/ Distributed Ledger Technology	Task Offloading, Cost of Execution, Local Loss Function	HEV-LFDO optimizes task offloading and resource management while securing BC data, minimizing local loss
[36]	IoT, WSN, FL, PSO	Packet Delivery Ratio, Average Delay, Throughput, Energy Efficiency	The proposed approach exhibited enhanced outcomes compared to existing solutions
[37]	BC Technology, LMDS	Computational Overhead and Time, Authentication Accuracy	The proposed LMDS technique effectively identifies malicious behaviour with minimal time
[38]	IoT, SqueezeNet, Squeeze_FDBO, DBO, FC, LadderNet	Accuracy, Sensitivity, Specificity, Negative Predictive Value, Positive Predictive Value, Routing Energy, Routing Distance, Routing Delay	The proposed Squeeze_FDBO method achieves high classification accuracy and better routing performance than existing methods
[39]	DL, BC, CNN, Cryptography-based FL	Classification Accuracy, Performance Comparison	The presented model outperforms existing techniques in classification and performance
[40]	BBOA, SNDAE, Min-Max Normalization	Accuracy, Sensitivity, Precision, Specificity, Negative Predictive Value, F-measure	The BBOA-SNDAE model outperforms existing models with high accuracy, precision, sensitivity, and specificity in HD prediction
[41]	IoT, CNN, Hyperparameter Adjustment	Classification Accuracy, Tumor Detection Rate	The proposed model attained 95% accuracy in tumour detection, enhancing breast cancer diagnosis and potentially reducing mortality through early detection
[42]	DL, IoT, Wearable Health Sensors, IoT Networking Systems	Patient Monitoring, Clinical Outcomes, Data Security	DL and IoT integration improve ICU patient care, enabling continuous monitoring, predictive analysis, and remote consultations while detecting opportunities for future research

Table 1. Summary of existing studies on load-balancing model.

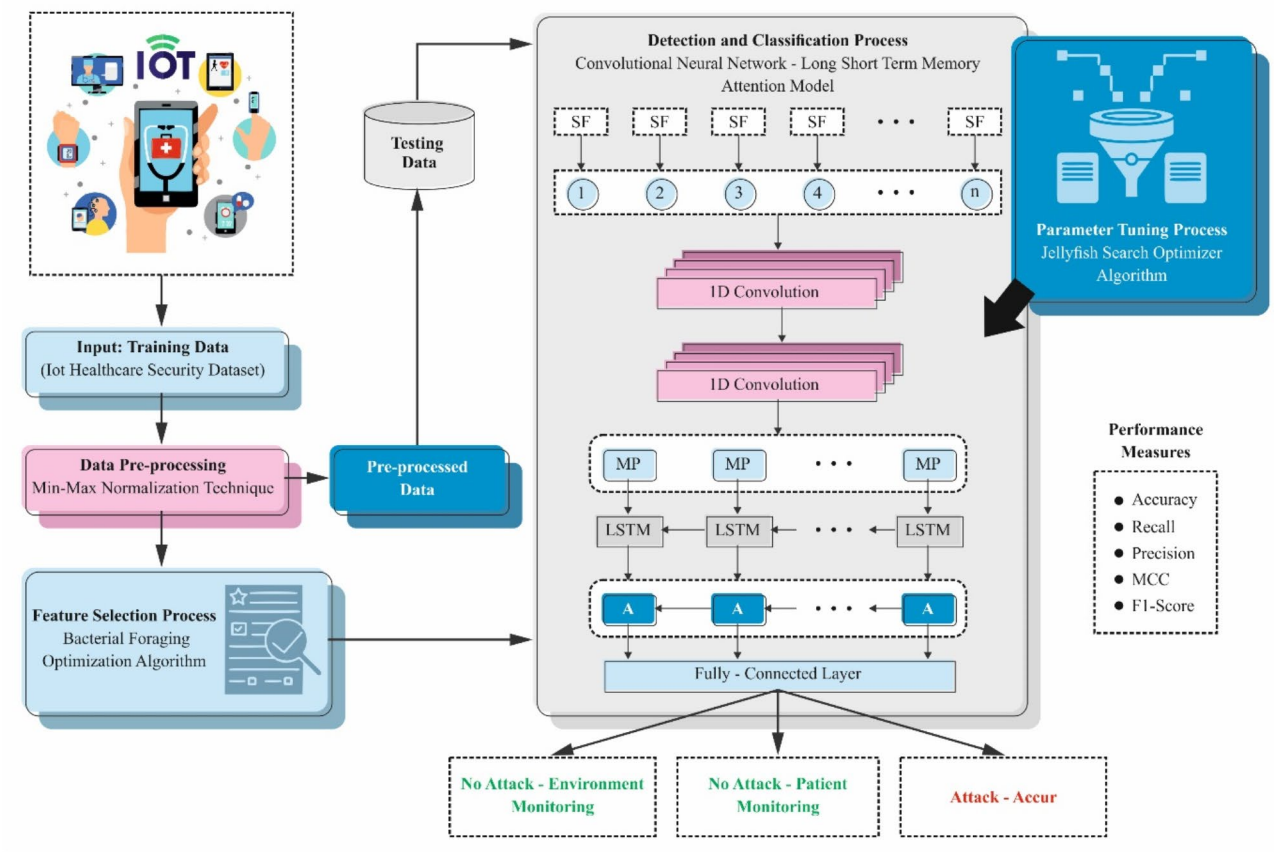

Fig. 2. Workflow of ESHCS-DLJSO technique.

Min-Max normalization

Primarily, the ESHCS-DLJSO method utilizes the min-max normalization model to measure the input data in a beneficial format[43]. Min-max normalization is a widely used pre-processing model due to its simplicity and efficiency in scaling input data to a fixed range, typically [0, 1]. This makes it specifically useful for ML models sensitive to the data's scale, such as neural networks and distance-based methods like k-nearest neighbours. By transforming all features to the same scale, min-max normalization assists in enhancing the convergence speed of gradient-based algorithms. It confirms that no single feature dominates the learning process due to differences in magnitude. Unlike standardization, which can result in a distribution with a mean of 0 and variance of 1, min-max normalization preserves the original distribution and makes it easier to interpret the data. Additionally, this model is computationally effective and works well when the data does not contain extreme outliers, offering a straightforward solution for preparing data for model training. Min-max normalization ensures consistency and accuracy and standardizes sensor data in patient monitoring. This method measures data to a specific range, typically [0, 1], enabling the analysis and integration of dissimilar health metrics from wearable devices. The normalization formulation is:

$$X' = \frac{X - X_{min}}{X_{max} - X_{min}} \tag{1}$$

Here, X denotes a value of original data; X_{min} and X_{max} represent the minimum and maximum values in the dataset, respectively; and X' means normalized value. This certifies that every sensor data is on a similar measure, improving the consistency of health assessments over HMI interfaces.

Feature selection using BFOA

Next, BFOA selects features. The BFOA is a population-based stochastic optimizer model stimulated by the foraging behaviour of Escherichia coli (E. coli) bacteria[44]. The BFOA is a bio-inspired optimization technique modelled after the foraging behaviour of bacteria, making it specifically effectual for feature extraction in intrinsic, high-dimensional datasets. Unlike conventional methods, namely genetic algorithms (GA) or PSO, BFOA utilizes a more robust search mechanism with local and global exploration capabilities, which helps prevent premature convergence to suboptimal solutions. Its iterative search process allows for the extraction of the most relevant features by balancing exploration and exploitation, thus confirming optimal feature selection in massive datasets. Furthermore, the capability of the BFOA model to handle noisy data and its flexibility in dealing with diverse feature types make it appropriate for healthcare and bioinformatics applications, where data can be heterogeneous and uncertain. Compared to other methods, BFOA is computationally effectual and presents enhanced accuracy in feature extraction, particularly in systems with multiple features and complex relationships. Figure 3 illustrates the working flow of the BFOA model.

Let the population of bacteria contain S numbers, and the current chemotactic, reproductive, and elimination-dispersal steps are signified by t, r, and e, correspondingly. At the tth chemotactic step, rth reproduction, and eth elimination dispersal, the nth bacterium's position in the D-dimension search space is denoted below:

$$\theta^{n}(t, r, e) = \left\{\theta^{1}_{n}(t, r, e) + \theta^{2}_{n}(t, r, e), \ldots\ldots, \theta^{D}_{n}(t, r, e)\right\} \tag{2}$$

The major procedures that take place in BFOA, including swarming, chemotaxis, elimination-dispersal, and reproduction, are defined in short below:

Chemotaxis

It is a procedure by which bacteria direct their environment in response to chemical gradients. This behaviour permits them to find favourable conditions like food sources. Bacteria attain chemotaxis over short runs (swims) and tumbles. Flagellar rotation defines their drive: swimming in a definite way or tumbling to discover novel regions. A unit-length arbitrary vector of direction defined in Eq. (3) demonstrates a tumble for the nth bacterium at the tth chemotactic, rth reproductive, and eth elimination dispersal steps. This vector defines the direction variation after a tumble.

$$\phi(i) = \frac{\Delta_i(t, r, e)}{\sqrt{\Delta_i^{T}(t, r, e)\,\Delta_i(t, r, l)}} \tag{3}$$

$$\theta^{n}(t+1, r, e) = \theta^{n}(t, r, e) + C(i)\,\phi(i) \tag{4}$$

whereas $\theta^{n}(t+1, r, e)$ signifies the nth bacterium at the tth chemotactic step, rth reproductive, and eth elimination dispersal step. $C(i)$ refers to the size of the step seized in the arbitrary direction definite by the tumble (the run length unit), and $\Delta_n(t, r, e)$ represents a randomly produced direction vector that defines the movement of the nth bacterium.

Swarming

Group behaviour in bacteria helps them drive near regions with greater nutrient attention. This phenomenon is demonstrated by presenting an extra cost function term (J) that affects every bacterium's proficient cost function (J). The swarming cost (J) considers the local bacterial density and the distance among distinct bacteria. The accurate representation of the swarming procedure is conveyed in Eq. (5):

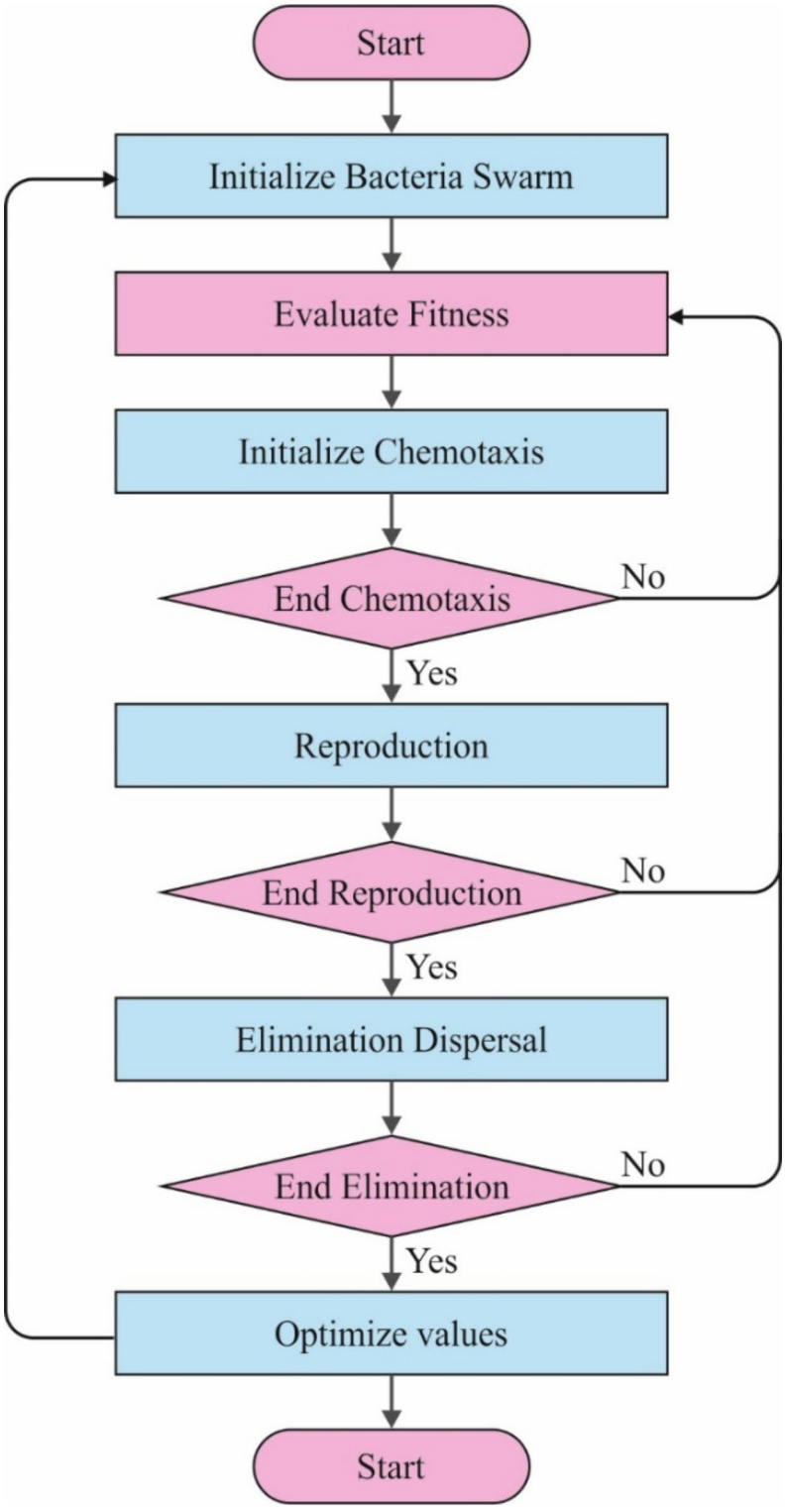

Fig. 3. Working flow of the BFOA method.

$$\begin{aligned} \mathrm{J}_{CC}(\theta, P(\mathrm{t}, \mathrm{re}) &= \sum {}_{n=1}^{s} j_{cc}^{n}\left(\theta, \theta^{n}(\mathrm{t}, \mathrm{re})\right) \\ &= \sum {}_{n=1}^{s}\left[-d_{attract} \exp\left(-\omega_{attract} \sum {}_{n=1}^{m}\left[\!\left[\left(\theta_{n}-\theta^{n}\right]\!\right]\right)^{2}\right)\right] \\ &+ \sum {}_{n=1}^{s}\left[h_{repellant} \exp\left(-\omega_{repellant} \sum {}_{n=1}^{m}\left[\!\left[\left(\theta_{n}-\theta^{n}\right]\!\right]\right)^{2}\right)\right] \end{aligned} \tag{5}$$

The related coefficients $(d_{attract}, \omega_{attract}, h_{repellant}\ and\ \omega_{repellant})$ influence the relative significance of swarming equal to the original cost function (J). These coefficients should be carefully preferred or adjusted to attain optimum performance in the BFOA.

Reproduction

Reproduction stage occurs after tracking a predefined integer of chemotactic steps (Nc). This stage helps the spread of "fitter" bacteria within the population. Bacteria with high health value, usually defined by a fitness function (FF), have a more significant opportunity of reproducing. On the other hand, bacteria with low health value will be removed. This mechanism certifies a constant size of the population while choosing individuals with improved foraging skills. The bacterium health value attained is given as follows:

$$J_{health}^{i} = \sum {}_{t=1}^{Nc} \mathrm{J}(\mathrm{n}, \mathrm{t}, \mathrm{r}, e) \tag{6}$$

Elimination-dispersal

It simulates the dynamic nature of the bacterial atmosphere, where local events can severely affect the population of bacteria. This procedure can remove every bacteria in a regional area and separate them into novel positions, possibly disturbing chemotaxis growth. It can also help search by assigning bacteria near latent food resources.

The FF reflects the classifier accuracy and the quantity of nominated features. It exploits the classifier accuracy and reduces the set dimension of certain features. Consequently, the FF mentioned below is employed to appraise distinct solutions, as exposed in Eq. (7).

$$Fitness = \alpha * ErrorRate + (1-\alpha) * \frac{\#SF}{\#All\_F} \tag{7}$$

Here, $ErrorRate$ indicates the classifier rate of error utilizing the nominated features. It is computed as the percentage of improperly categorized to the number of classifications prepared, conveyed as a value between 0 and 1. ($ErrorRate$ is the complement of the classifier accuracy), $\#SF$ is the number of chosen features, and $\#All\_F$ denotes the total number of attributes in the original dataset. α is employed to switch the position of classification excellence and sub-set length. In the experiments, α is set to 0.9.

Detection method using CNN-LSTM-Attention model

Furthermore, the CNN-LSTM-Attention method is used for disease detection and classification[45]. This technique is an efficient choice for disease detection and classification due to its capability to utilize the merits of both convolutional and recurrent networks, integrated with the power of attention mechanisms. CNNs outperform at extracting spatial features from medical images or time-series data, capturing local patterns and hierarchical structures. LSTMs, on the contrary, are appropriate for sequential data, such as time-series medical signals, enabling the technique to capture long-term dependencies and temporal patterns. The incorporation of attention mechanisms allows the model to concentrate on the most relevant features of the input, improving interpretability and enhancing performance by accentuating significant data points while ignoring irrelevant data. This integration is beneficial in healthcare, where medical data is often noisy, complex, and high-dimensional. Compared to conventional techniques such as SVM or shallow neural networks, the CNN-LSTM-Attention model gives superior accuracy, robustness, and the ability to handle diverse data types, making it highly effective for disease detection and classification tasks. Figure 4 depicts the structure of the CNN-LSTM-Attention technique.

A CNN has been broadly employed as a feed-forward neural network (FFNN), mainly collected of fully connected layers (FCL), convolutional layers (CL), and pooling layers (PL). The layer counts are fine-tuned based on the method requirements. The main concept for a CNN is convolutional actions for managing information in Euclidean space, thus providing considerable benefits. In CNNs, the CL is mainly applied for extracting features by benefits like spatial invariance, local perception, and weight sharing. The PL has been used to reduce the data dimensionality once convolutional actions inhibit over-fitting. Regular approaches contain $\mathrm{average}$ and $\max$ pooling. The FCL maps the removed features and permits them to be used as a classifier for regression or classification. This work used a one-dimensional CNN using convolutional kernels. The objective is to capture features and share parameters, decreasing the parameter counts required for model optimizer and computational complexity. This method improves the model's training scalability and efficiency.

LSTM networks are advanced depending on conventional RNNs, presenting gating methods to help moderate the problems of exploding and vanishing gradients, which RNNs face after handling long-term dependency. The network form of an LSTM technique contains 3 gate elements: the input gate, the output gate, and the forget gate. The forget gate is critical in guiding the amount of data transmitted from earlier to the present state. Simultaneously, the input gate moderates the effect of recently obtained data on the existing state, and the output gate manages the dependence of the present output on the memory cell state. Also, the network filters maintain ancient data state without inserting novel input data. On the other hand, when the input gate methods value one

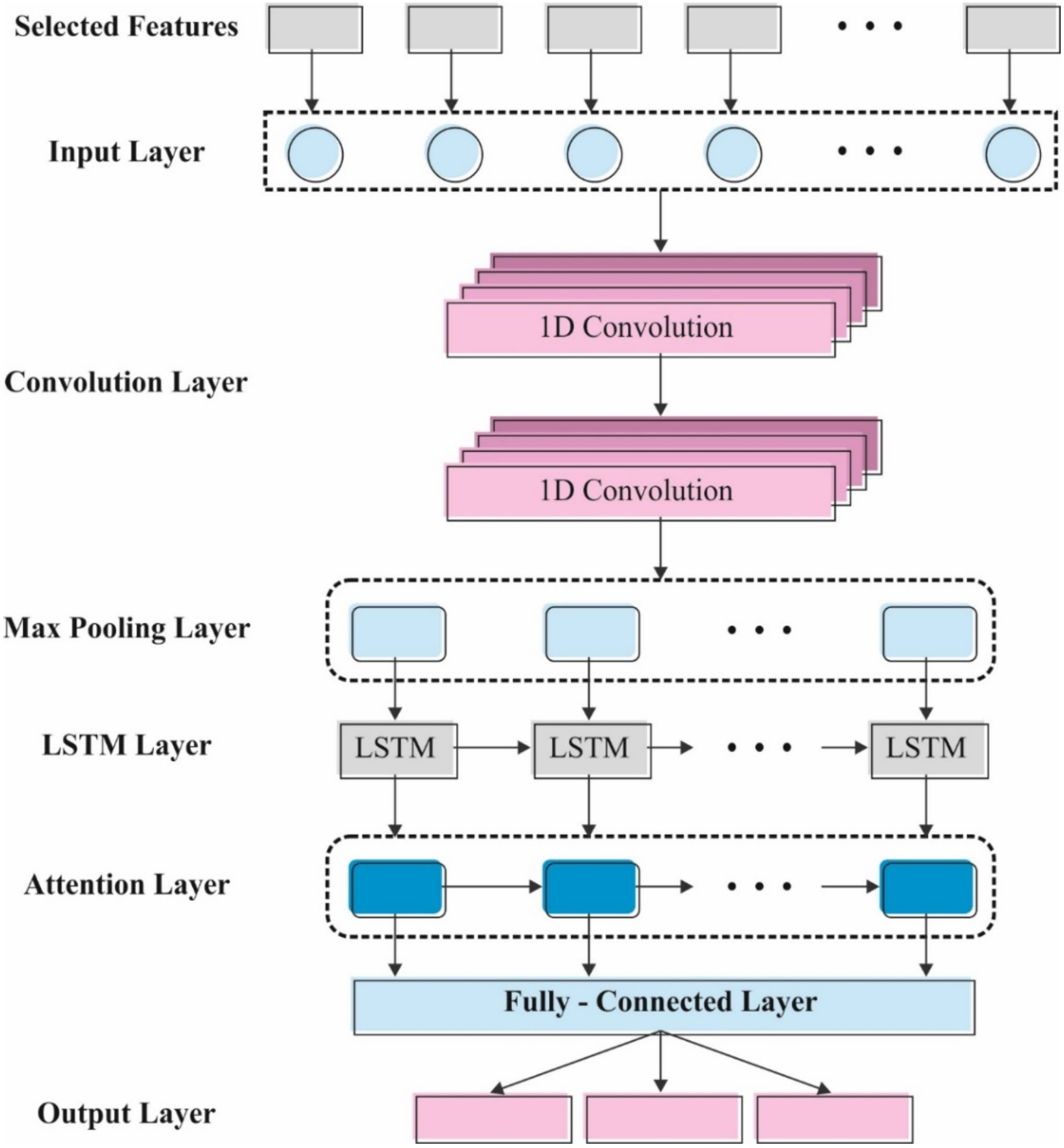

Fig. 4. Architecture of CNN-LSTM-attention model.

while the forget gate methods value 0, the LSTM network attains a memory upgrading function. This network dismisses ancient data irrelevant to the present task and concentrates on the present input data.

The collaboration method amongst gates makes LSTM more adaptable in memory and learning. LSTM frequently exceeds the conventional RNN. The LSTM unit structure, with Eqs. (8)–(13) is described as follows:

$$i_t = \sigma\ (W_i x_t + U_i h_{t-1} + b_i) \tag{8}$$

$$f_t = \sigma\ (W_f x_t + U_f h_{t-1} + b_f) \tag{9}$$

$$o_t = \sigma\ (W_o x_t + U_o h_{t-1} + b_o) \tag{10}$$

$$\widetilde{C}_t = \tanh\ (W_c x_t + U_c h_{t-1}) \tag{11}$$

$$c_t = f_t \odot c_{t-1} + i_t \odot \widetilde{C}_{t-1} \tag{12}$$

$$h_t = o_t \odot \tanh(c_t) \tag{13}$$

whereas i_t, f_t, and o_t correspondingly relate toward switching states of the input, output, and forget gates; $\widetilde{C}_t$ exists the cell state of a candidate; c_t exists present cell state; h_t exists the present unseen state; x_t exists input sequence value at the present time-step; W and U signify the three gates weight matrices; b denotes the bias vector; and σ characterizes the activation function of sigmoid, whereas $\tanh$ means the hyperbolic activation function of tangent. The CNN-LSTM approach is broadly applied. Nevertheless, its performance can be narrowed by optimizer methods. Methods can overwhelm this limitation by presenting attention methods that imitator the human brain's data handling and considerably increase neural networks' capacity for managing spatial and temporal information. These lead to improved optimization model performances and generalization.

Attention has been theorized as a weighted summation, whereas the weights relate to the correspondence among the vectors of calculation. The first attention contains Q, K, and V from input features. V signifies the input feature vectors, and Q and K are feature vectors applied to estimate the attention weights. If an attention network is not presented, then a single set of V is required to input it for training the network. Nevertheless, once an attention network was given, those groups of V needed to be multiplied by a group of weights $F(Q, K)$, allowing the network to concentrate on limited features of the input.

Initially, attention scores are gained by computing the correlation or similarity between a keyword (Key) and query, with usual approaches such as additive attention, scaled dot product, and dot product. Next, the softmax function controls the attention scores, transforming them into a probability distribution, which characterizes each value's importance. Lastly, the values are summed and weighted based on the normalized attention scores with a weighted sum method. This results in a weighted average representation, highlighting data related to the query Eqs. (14)–(16) are utilized to achieve this constraint:

$$s_i = F(Q, k_i) \tag{14}$$

$$\alpha_i = softmax(s_i) = \frac{\exp(s_i)}{\sum_{j=1}^{N} \exp(s_j)} \tag{15}$$

$$Attention((K, V), Q) = \sum_{i=1}^{N} \alpha_i v_i \tag{16}$$

Hyperparameter tuning process

Finally, the hyperparameter tuning method is performed using the JSO method. The JSO model simulates the movement of jellyfish in the water[46]. This is an effectual global optimization algorithm inspired by the social behaviour of jellyfish, making it specifically effectual for hyperparameter tuning in intrinsic ML techniques. Unlike traditional approaches such as grid search or random search, JSO gives a more dynamic and adaptive approach, exploring the search space more thoroughly while balancing exploration and exploitation. The capability of the JSO model to escape local optima confirms that it can find improved hyperparameter combinations, enhancing model performance and generalization. It has proven to be computationally efficient and less prone to overfitting related to other optimization methods, namely GA or PSO. Additionally, JSO works well in high-dimensional search spaces, making it ideal for tuning DL methods with various hyperparameters. This makes JSO a robust choice for enhancing the accuracy and effectualness of models in fields like healthcare, where hyperparameter optimization is significant for attaining high-quality predictions. Figure 5 demonstrates the overall workflow of the JSO methodology.

The JSO model includes key modules like passive and active motions, ocean currents, a group of jellyfish, and a time control device. These vital rubrics for the proposed optimization technique can be summarized as below:

Ocean current

The jellyfish are appealed to nutrients that are in the water present. The movement of the ocean current $\left(\overrightarrow{trend}\right)$ is established by averaging every vector from every jellyfish in the sea to the finest jellyfish:

$$\overrightarrow{trend} = \frac{1}{n_{pop}} \sum trend_i = \frac{1}{n_{pop}} \sum (X_{best} - e_c X_i)$$

$$= X_{best} - e_c \frac{\sum X_i}{n_{pop}} X^* - e_c \mu = X_{best} - df$$

$$df = e_c \mu$$

$$e_c = \beta * rand(0,1)$$

$$df = \beta * rand(0,1) * \mu \tag{17}$$

whereas df signifies the difference between every jellyfish's mean position and the jellyfish's present finest position, while n_{pop} signifies the number of jellyfish in the ocean, X_{best} denotes the finest position; e_c

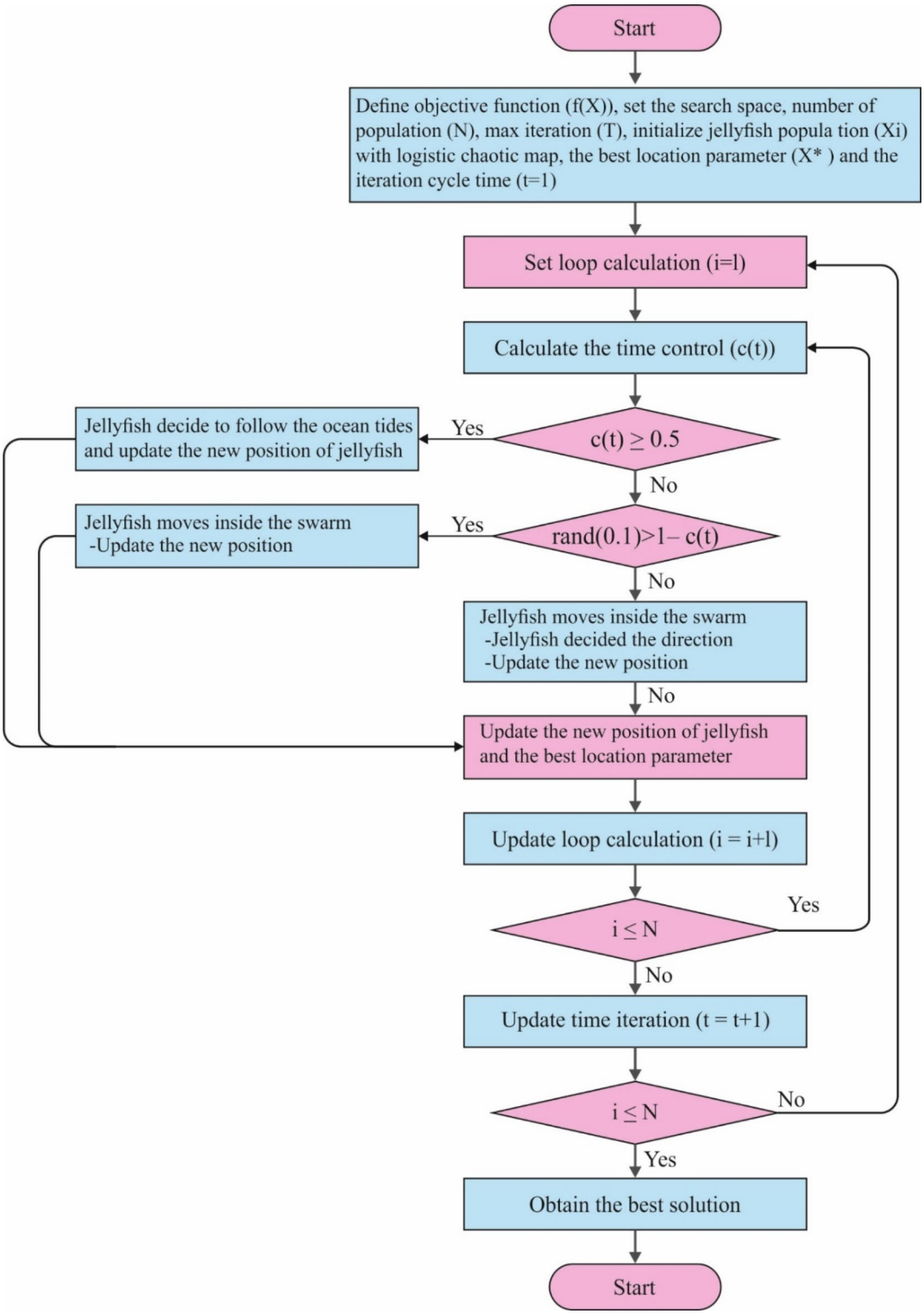

Fig. 5. Workflow of the JSO technique.

represents the factor which controls the attraction. μ denotes the average location of every jellyfish. The novel location of every jellyfish is numerically computed below:

$$X_i(t+1) = X_i(t) + rand(0,1) * \overrightarrow{trend}, \tag{18}$$

It is intended by

$$X_i\,(t+1) = X_i\,(t) + rand\,(0,1) * (X_{best} - \beta\ * rand\,(0,1)\,\mu\,) \tag{19}$$

whereas $\beta\ > 0$ means a distribution parameter accompanied by the distance of $\overrightarrow{trend}$.

Group of jellyfish

In the Jellyfish group, dual dissimilar kinds of motions can be detected. The 1st type is recognized as Type A, which resembles passive motion, while the 2nd type, denoted as Type B, signifies active motion. As the group was initially made, the jellyfish showed mainly Type A motion, slowly progressing into Type B. Type A motion includes the jellyfish affecting around their particular positions, and the upgraded location of every jellyfish is computed utilizing the below-mentioned formulation:

$$X_i(\mathcal{J}+1) = X_i\,(\mathcal{J}) + \gamma\ * rand\,(0,1) * (U_b - L_b) \tag{20}$$

Meanwhile, U_b and L_b denote the upper and lower limits. The coefficient of motion is $\gamma\ > 0$, related to the movement of jellyfish regarding their locations.

In the swarm of jellyfish, a set of jellyfish (j) and (i) are randomly preferred. If the size of food at the location of jellyfish (j) is larger than the food dimension at the position of the target jellyfish (i), then the target jellyfish (i) will travel near the location of jellyfish (j). On the other hand, if the size of the food set for the preferred jellyfish (j) is lesser than the food size arranged for the target jellyfish (i), then the target jellyfish (i) will go straight away from it. This procedure certifies that every jellyfish in the group alters its location depending upon the most effectual model of attaining food.

$$\overrightarrow{step} = X_i(t+1) - X_i\,(t) \tag{21}$$

where, $\overrightarrow{step} = rand\,(0,1) * \overrightarrow{direction}$

$$\overrightarrow{direction} = \begin{cases} X_j\,(t) - X_i\,(t) & if\ f\,(X_i) \geq\ f\,(X_j) \\ X_i\,(t) - X_j\,(t) & if\ f\,(X_i) < f\,(X_j) \end{cases} \tag{22}$$

Meanwhile, $f\,(X_i)$ signifies an objective function.

Henceforth, $X_i(t+1) = \overrightarrow{step} + X_i\,(t)$.

The time control technique is used to portray the motion pattern over time, particularly with the drive of jellyfish within an ocean current. It rules how the jellyfish cross across the current.

Time control mechanism

The time control mechanism is presented to normalize the jellyfish's movement within the group and their navigation under the sea current. This method covers a constant C_0 and a time control function $C\,(t)$. $C\,(t)$ is positioned at random among 0 and 1.

$$C\,(t) = \left| \left(1 - \frac{t}{\mathrm{Max\_}it}\right) * (2 * rand\,(0,1) - 1) \right| \tag{23}$$

The JSO method originates an FF to achieve an enhanced classifier solution. It states a positive number to denote the enhanced efficiency of the candidate solution. In this paper, the minimizer of the classifier error rate is regarded as FF and formulation is expressed in Eq. (24).

$$\begin{aligned} fitness\,(x_i) &= ClassifierErrorRate\,(x_i) \\ &= \frac{no.\ of\ misclassified\ samples}{Total\ no.\ of\ samples} \times\ 100 \end{aligned} \tag{24}$$

Result analysis

The simulation validation of the ESHCS-DLJSO technique was verified on the IoT healthcare security dataset[47]. It has been made a use case of an IoT-based ICU with a volume of 2 beds, whereas all beds are set with nine patient monitoring devices (i.e., sensors) and one control unit named Bedx-Control-Unit. Each of these devices was generated using the IoT-Flock tool. The original dataset contains 50 features; the top 24 features are chosen, namely frame.time_delta, frame.len, ip.src, ip. dst, tcp. dstport, tcp. flags, tcp.len, tcp.ack, tcp.connection.fin, tcp. flags.ack, tcp. flags.push, tcp.flags.urg, tcp.checksum, mqtt.clientid, mqtt.conack.flags, mqtt.conack.val, mqtt.conflag.qos, mqtt.conflag.retain, mqtt.hdrflags, mqtt.kalive, mqtt.retain, mqtt.topic, mqtt.ver, ip.proto. The dataset comprises 30,000 samples under three classes. Each class contains 10,000 samples, as represented in Table 2.

Figure 6 shows a collection of confusion matrices made by the ESHCS-DLJSO approach on diverse epoch counts. The confusion matrix provides a detailed breakdown of the classification performance at different epochs (500, 1000, 1500, 2000, 2500, and 3000). It illustrates the true positive (TP), false positive (FP), false negative (FN), and true negative (TN) rates for three classes: Class 0, Class 1, and Class 2. As the epochs increase, the model consistently enhances its performance across all classes, with TP rates nearing 99% and FN rates remaining low. For example, at Epoch 500, Class 0 has a TP of 98.06%, and at Epoch 3000, Class 2 has a TP of 99.16%. The FN and FP rates decrease with higher epochs, demonstrating the improved accuracy and efficiency

Class labels	Class names	Samples
Class 0	No attack-environment monitoring	10,000
Class 1	No attack-patient monitoring	10,000
Class 2	Attack-Accur	10,000
Total no. of samples		30,000

Table 2. Details on dataset.

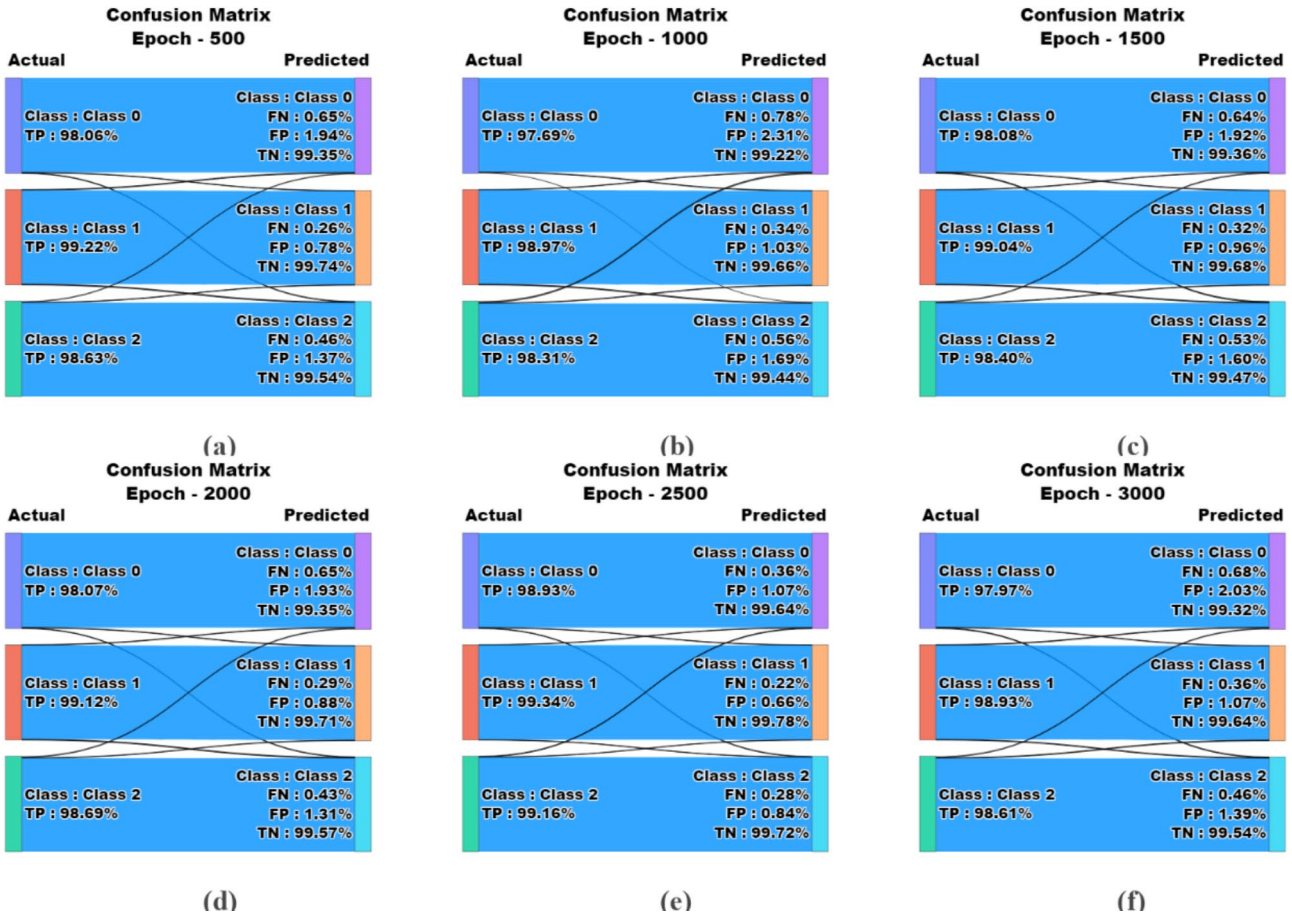

Fig. 6. Confusion matrices of ESHCS-DLJSO technique (a-f) Epochs 500–3000.

of the model as training progresses. The results identify that the ESHCS-DLJSO method efficiently recognizes samples under all three class labels.

Table 3 offers the recognition result of the ESHCS-DLJSO approach under different epoch counts.

Figure 7 displays the average result of the ESHCS-DLJSO method under 500–1500 epochs. The figure values reported that the ESHCS-DLJSO process accurately recognized all three samples. On 500 epoch counts, the ESHCS-DLJSO models present an average $accu_y$ of 99.09%, $prec_n$ of 98.64%, $reca_l$ of 98.63%, $F1_{score}$ of 98.63%, and MCC of 97.95%. Moreover, on 1000 epoch counts, the ESHCS-DLJSO approach provides an average $accu_y$ of 98.88%, $prec_n$ of 98.32%, $reca_l$ of 98.32%, $F1_{score}$ of 98.32%, and MCC of 97.48%.

Figure 8 demonstrates the average outcome of the ESHCS-DLJSO method under 2000–3000 epochs. The figure values reported that the ESHCS-DLJSO process accurately recognized all three samples. In the meantime, on 2000 epoch counts, the ESHCS-DLJSO process attains an average $accu_y$ of 99.08%, $prec_n$ of 98.63%, $reca_l$ of 98.62%, $F1_{score}$ of 98.62%, and MCC of 97.94%. Additionally, on 3000 epoch counts, the ESHCS-DLJSO techniques provide an average $accu_y$ of 99.00%, $prec_n$ of 98.50%, $reca_l$ of 98.50%, $F1_{score}$ of 98.50%, and MCC of 97.75%.

In Fig. 9, the training and validation accuracy outcomes of the ESHCS-DLJSO methods under different epoch counts are portrayed. The precision values are computed for 0–3000 epoch counts. This figure underlined that the training and validation accuracy values show a growing trend that informed the capacity of the ESHCS-DLJSO technique with better performance over numerous iterations. In addition, the training and validation

Class labels	$Accu_y$	$Prec_n$	$Reca_l$	$F1_{score}$	MCC
Epoch—500					
Class 0	99.02	98.06	99.03	98.54	97.81
Class 1	99.24	99.22	98.50	98.86	98.30
Class 2	99.00	98.63	98.37	98.50	97.75
Average	99.09	98.64	98.63	98.63	97.95
Epoch—1000					
Class 0	98.74	97.69	98.56	98.12	97.18
Class 1	99.25	98.97	98.77	98.87	98.30
Class 2	98.65	98.31	97.63	97.97	96.96
Average	98.88	98.32	98.32	98.32	97.48
Epoch—1500					
Class 0	98.92	98.08	98.68	98.38	97.57
Class 1	99.27	99.04	98.78	98.91	98.36
Class 2	98.82	98.40	98.06	98.23	97.35
Average	99.00	98.51	98.51	98.51	97.76
Epoch—2000					
Class 0	99.01	98.07	98.98	98.52	97.78
Class 1	99.30	99.12	98.79	98.95	98.43
Class 2	98.93	98.69	98.10	98.40	97.60
Average	99.08	98.63	98.62	98.62	97.94
Epoch—2500					
Class 0	99.34	98.93	99.09	99.01	98.52
Class 1	99.55	99.34	99.32	99.33	98.99
Class 2	99.39	99.16	99.02	99.09	98.63
Average	99.43	99.14	99.14	99.14	98.72
Epoch—3000					
Class 0	98.93	97.97	98.85	98.41	97.61
Class 1	99.24	98.93	98.78	98.85	98.28
Class 2	98.83	98.61	97.87	98.24	97.36
Average	99.00	98.50	98.50	98.50	97.75

Table 3. Detection outcome of the ESHCS-DLJSO model under distinct epochs.

accuracy stay nearer over the epoch counts, which point out the least minimum overfitting and display improved performance of the ESHCS-DLJSO technique, assuring consistent prediction on hidden samples.

Figure 10 presents the training and validation loss graph of the ESHCS-DLJSO approach under different epoch counts. The loss values are computed throughout 0–3000 epoch counts. It is denoted that the training and validation accuracy values imply a reducing trend, reporting the ability of the ESHCS-DLJSO technique to balance a trade-off between generalization and data fitting. The constant decrease in loss values also promises the improved performance of the ESHCS-DLJSO process and tunes the prediction outcomes in time.

In Fig. 11, the precision-recall (PR) curve examination of the ESHCS-DLJSO method under different epoch counts interprets its performance by plotting Precision against Recall for each class label. This figure shows that the ESHCS-DLJSO approach steadily obtained enhanced PR values over dissimilar classes, pointing out its capability to handle an essential segment of TP predictions between every positive prediction (precision) and capture many actual positives (recall). The constant growth in PR results between all class labels depicts the efficiency of the ESHCS-DLJSO techniques in the classification process.

In Fig. 12, the ROC curve of the ESHCS-DLJSO method was examined. The outcomes infer that the ESHCS-DLJSO approach, under different epoch counts, attains better ROC results across every class label, representing a critical ability to differentiate the class labels. These growing tendencies of better ROC values across numerous class labels denote the efficient performance of the ESHCS-DLJSO approach in predicting class labels, emphasizing the robust nature of the classification method.

Table 4; Fig. 13 compare ESHCS-DLJSO methods with existing studies[48–50]. The results identify that the ESHCS-DLJSO approach accurately identified all three samples. Compared with $accu_y$, the ESHCS-DLJSO models show their supremacy with a better $accu_y$ of 99.43%. At the same time, the XG-ABC, XG-COLSHADE, CNN-TSODE, RNN, CNN, FS-LSTM, and XSRU-IoMT processes gained lowered performance with $accu_y$ of 94.60%, 98.04%, 92.90%, 94.64%, 94.36%, 92.95%, and 98.39%, respectively. Moreover, equating with $prec_n$, the ESHCS-DLJSO techniques display its supremacy with a better $prec_n$ of 99.14%. In contrast, the XG-ABC, XG-COLSHADE, CNN-TSODE, RNN, CNN, FS-LSTM, and XSRU-IoMT processes acquire minimum performance with $prec_n$ of 94.22%, 91.87%, 91.63%, 97.15%, 93.79%, 93.78%, and 96.89%, respectively.

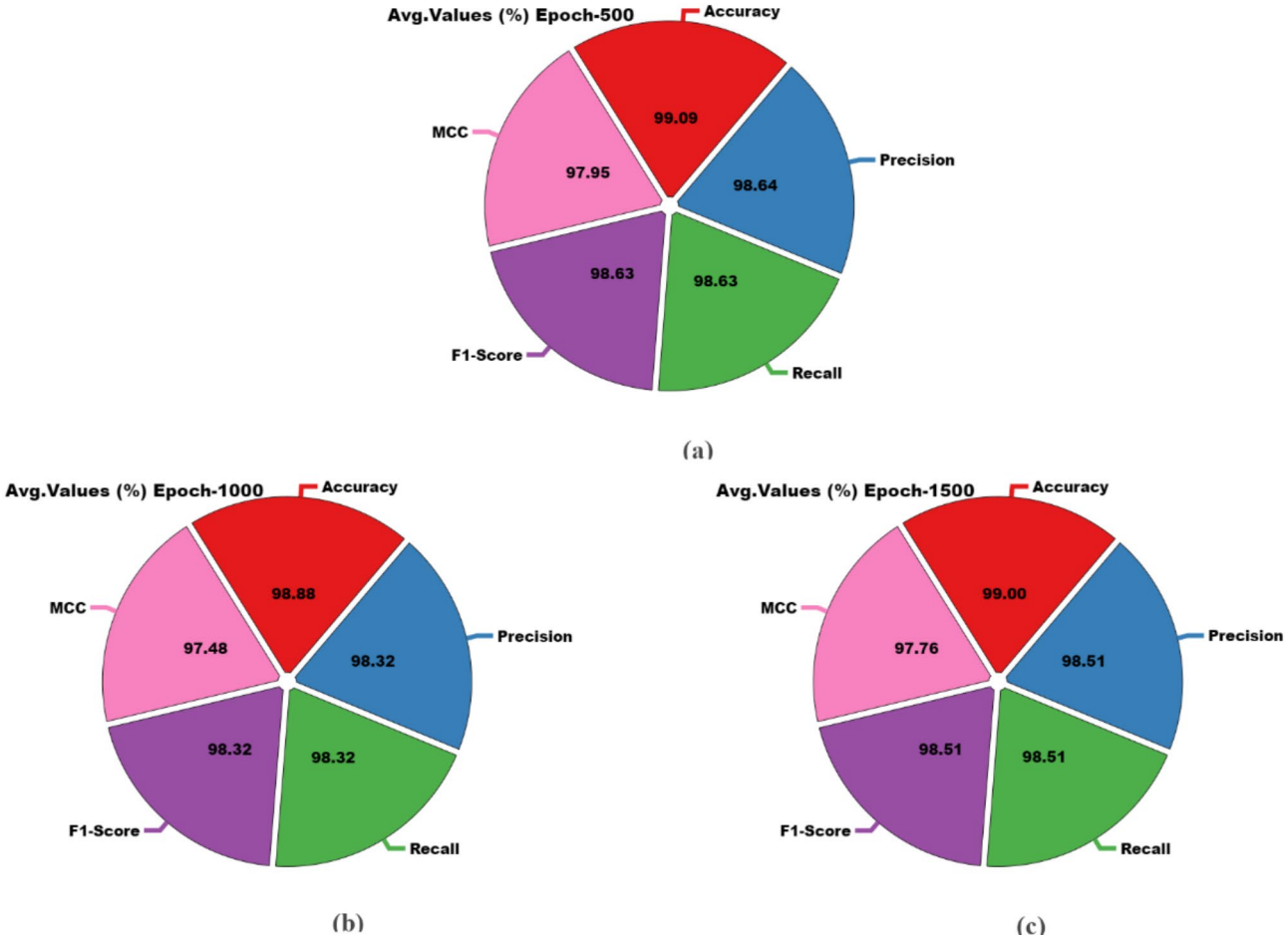

Fig. 7. Average outcome of ESHCS-DLJSO model (**a**–**c**) Epochs 500–1500.

Table 5; Fig. 14 specify the computational time (CT) analysis of the ESHCS-DLJSO technique with existing studies. The methods evaluated in terms of CT are as follows: XG-ABC took 5.98 s, XG-COLSHADE took 8.98 s, CNN-TSODE took 11.21 s, RNN took 8.64 s, CNN Classifier took 13.33 s, FS-LSTM took 5.88 s, XSRU-IoMT took 10.79 s, and ESHCS-DLJSO took 3.89 s.

Conclusion

In this study, an ESHCS-DLJSO technique for IoT healthcare applications is presented. This model comprises four distinct processes involving data normalization, BFOA-based feature selection, CNN-LSTM-Attention using disease detection process, and JSO-based parameter selection. Initially, the ESHCS-DLJSO model employs a min-max normalization technique to measure the input data into a beneficial format. In addition, BFOA accomplishes feature selection. Next, the ESHCS-DLJSO approach utilizes the CNN-LSTM-Attention model for disease classification and detection. Eventually, the JSO method is employed for the hyperparameter tuning process. The simulation of the ESHCS-DLJSO technique is examined on an IoT healthcare security dataset. The performance validation of the ESHCS-DLJSO technique portrayed a superior accuracy value of 99.43% over existing approaches. The limitations of the presented study comprise enhanced computational complexity with larger datasets, reliance on high-quality input data, and limited applicability to other diseases without additional adaptation. Furthermore, the models may need help with noisy or incomplete data and imbalanced datasets, which are common in healthcare. For future work, efforts can be directed toward enhancing the model's scalability to handle large-scale, real-time healthcare data streams. Moreover, exploring more robust data augmentation models to handle noisy, missing, or unbalanced data could improve the generalization and reliability of the model. Future studies could also investigate incorporating multi-modal data sources, such as integrating patient health records with wearable device data, to enhance diagnostic accuracy. Finally, exploring TL techniques to adapt the models to new diseases or healthcare contexts with minimal labelled data would improve the flexibility and usability of the model in diverse healthcare scenarios.

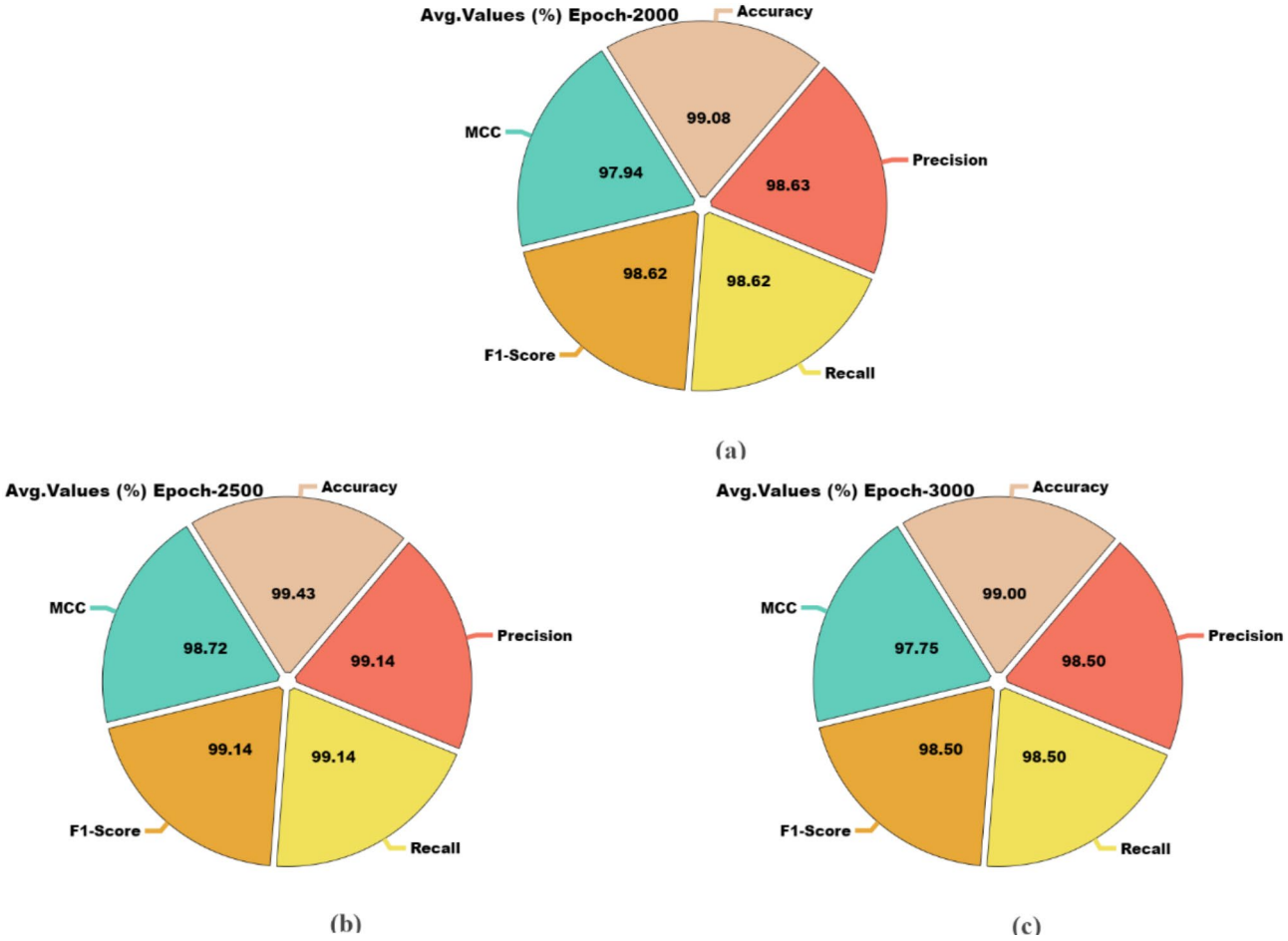

Fig. 8. Average outcome of ESHCS-DLJSO model (**a**–**c**) Epochs 2000–3000.

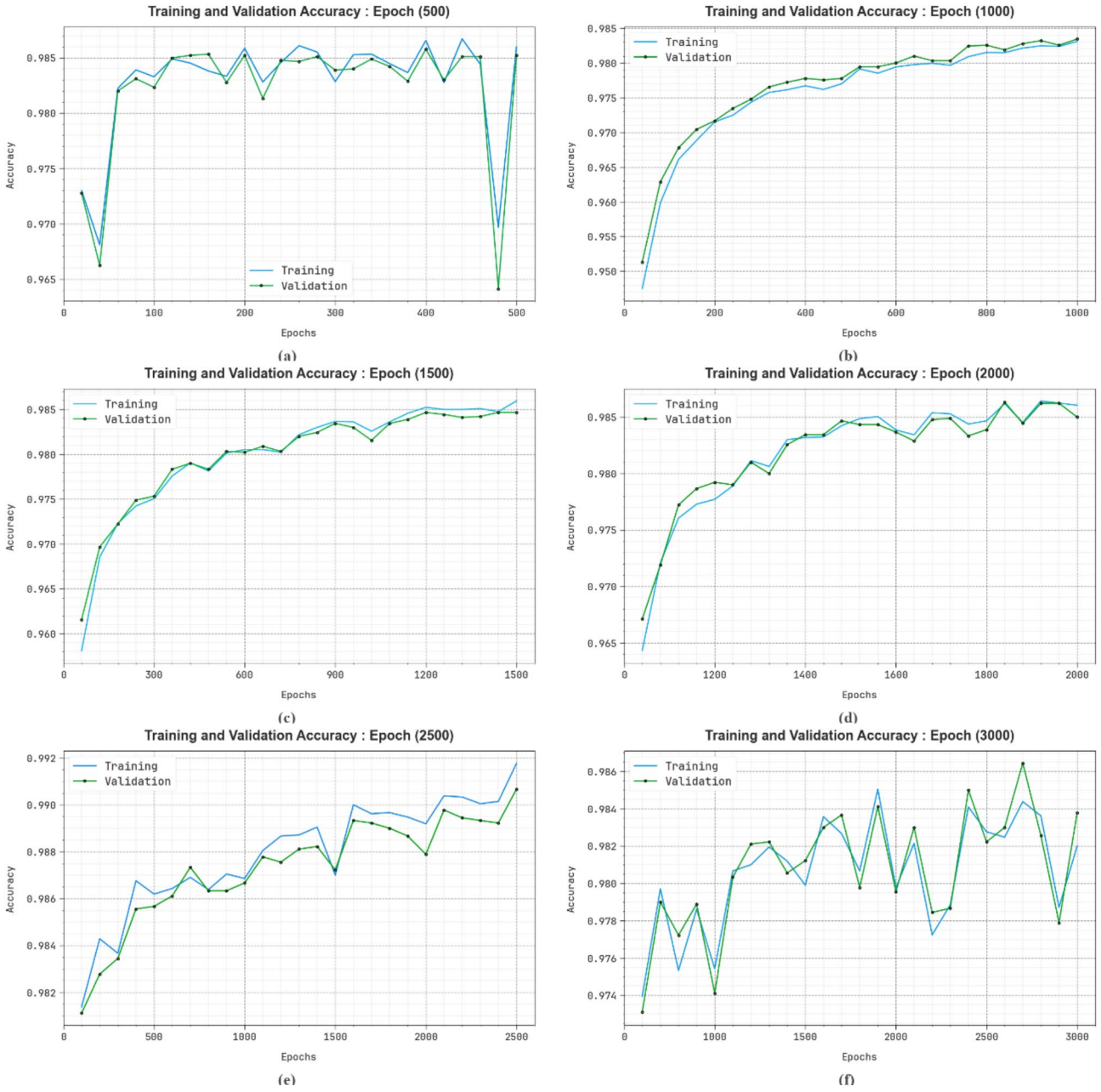

Fig. 9. $Accu_y$ curve of ESHCS-DLJSO technique (**a**–**f**) Epochs 500–3000

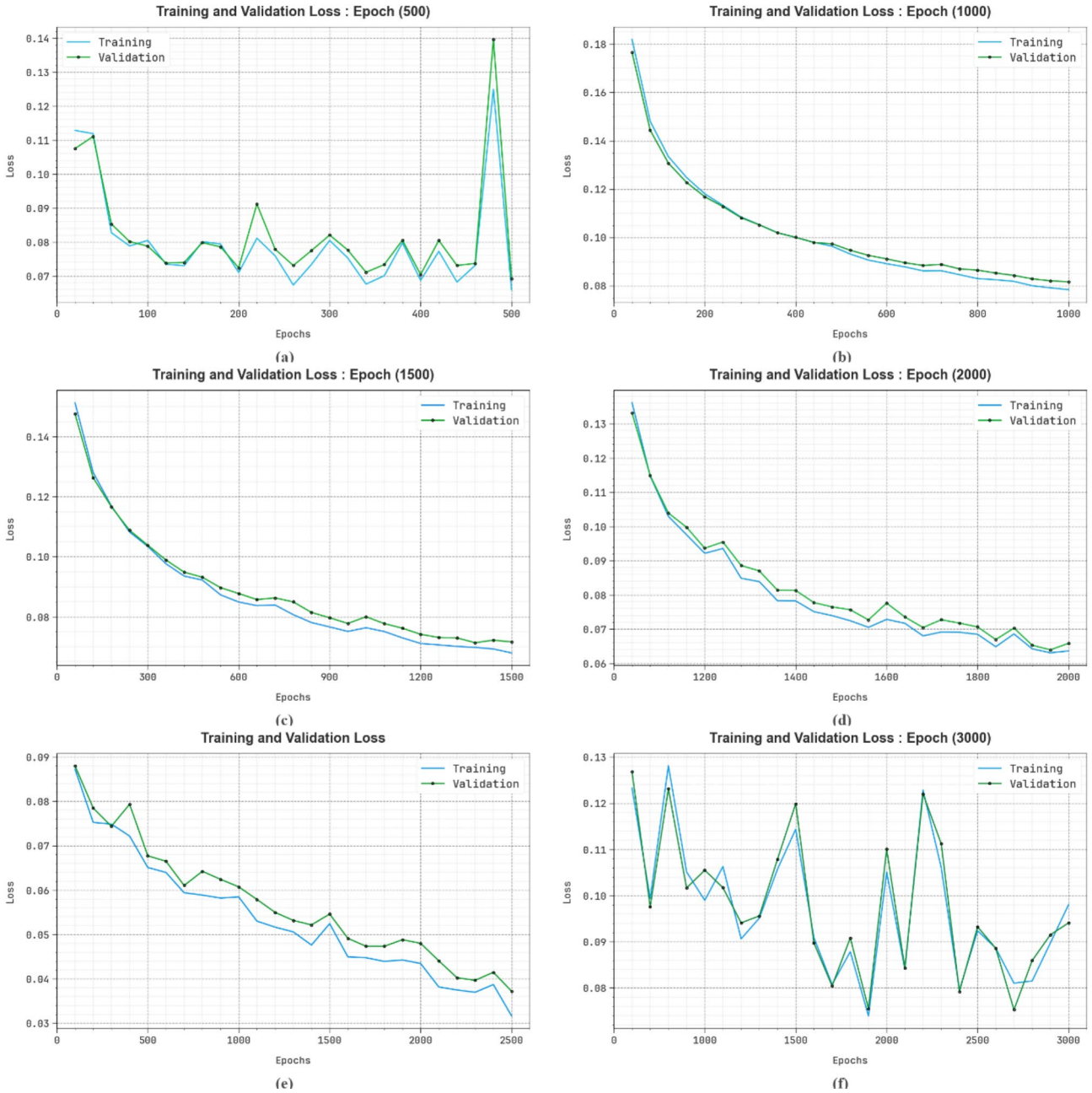

Fig. 10. Loss curve of ESHCS-DLJSO technique (**a**–**f**) Epochs 500–3000.

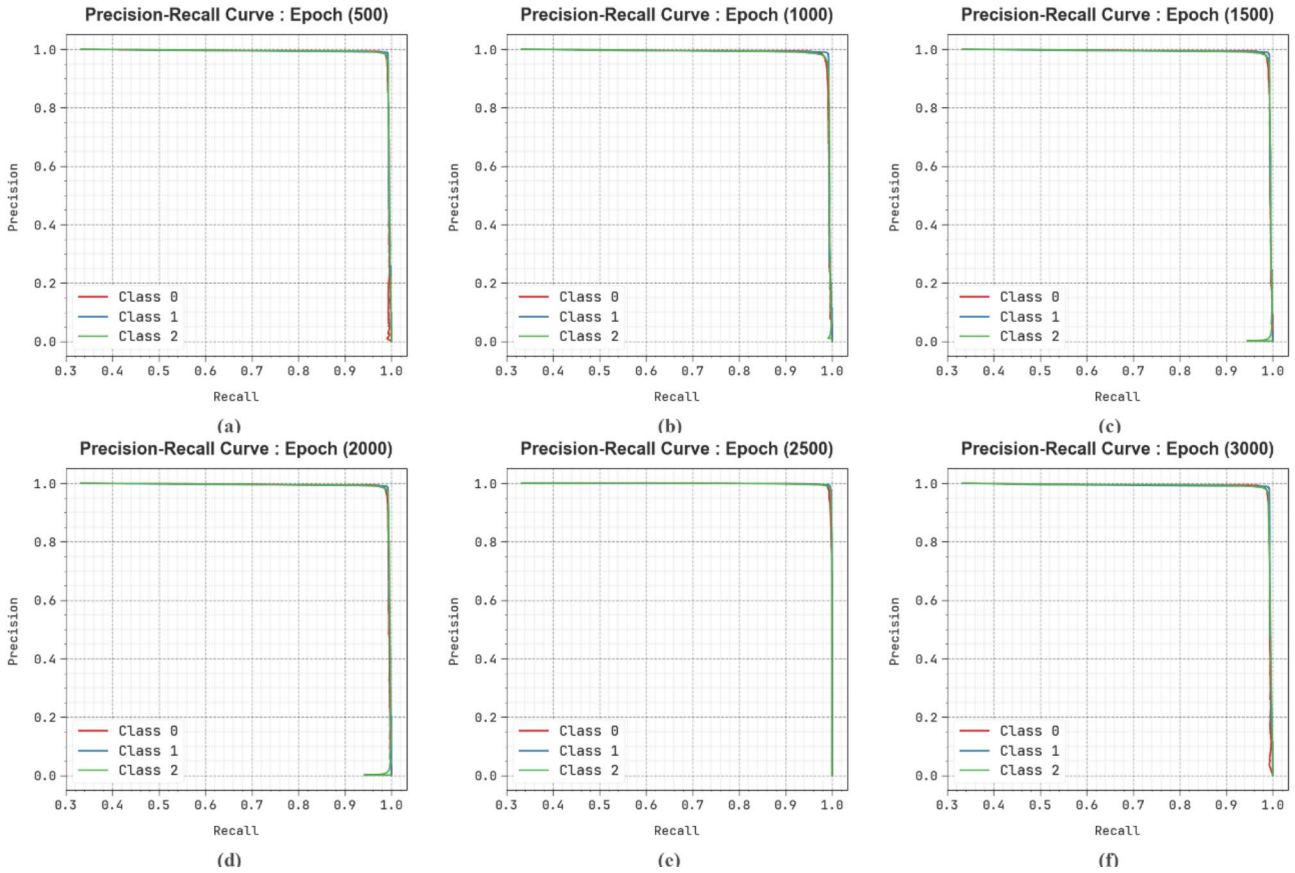

Fig. 11. PR curve of ESHCS-DLJSO technique (**a**–**f**) Epochs 500–3000.

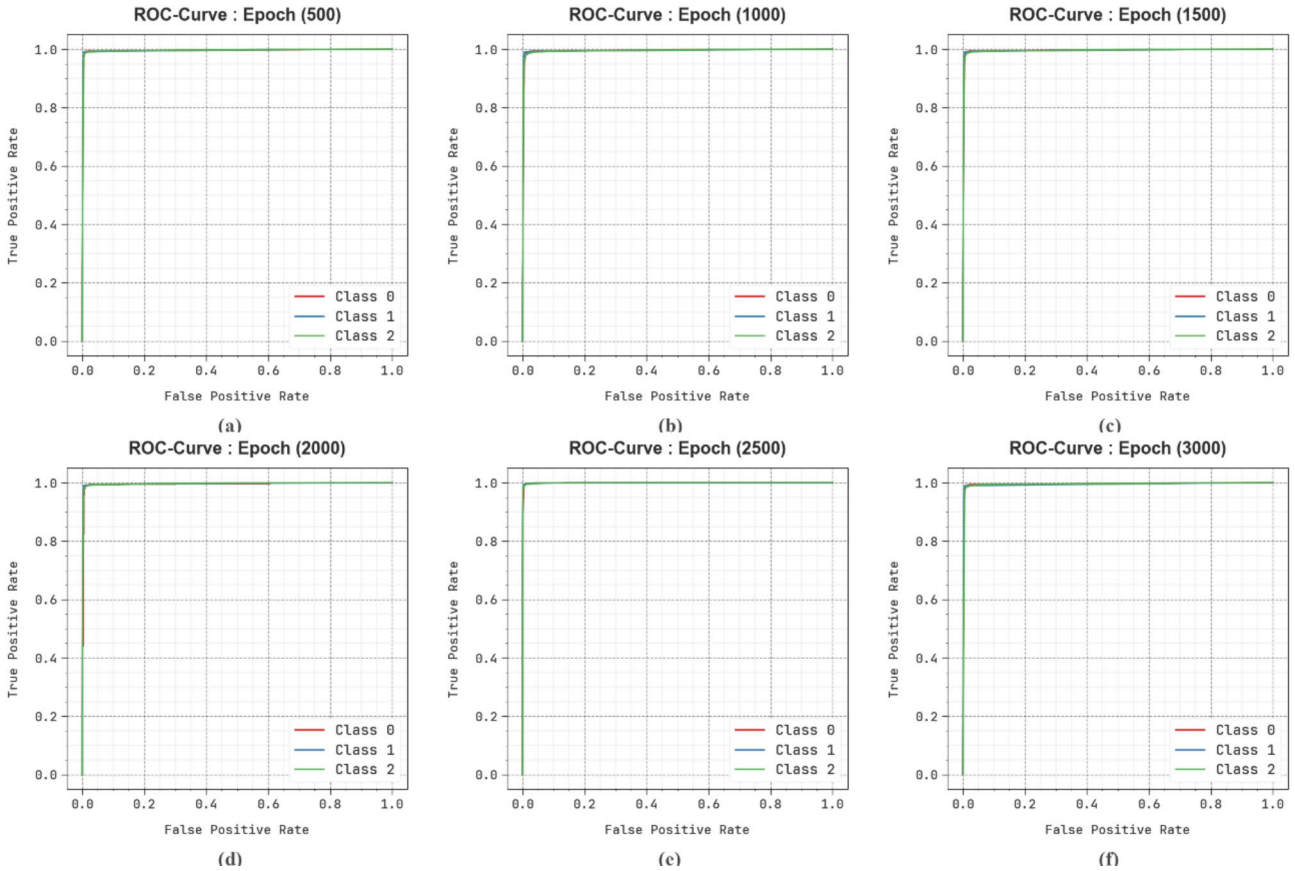

Fig. 12. ROC curve of ESHCS-DLJSO technique (**a**–**f**) Epochs 500–3000.

Method	$Accu_y$	$Prec_n$	$Reca_l$	$F1_{score}$
XG-ABC	94.60	94.22	94.74	95.87
XG-COLSHADE	98.04	91.87	96.92	92.35
CNN-TSODE	92.90	91.63	93.58	97.53
RNN	94.64	97.15	93.49	98.25
CNN Classifier	94.36	93.79	93.93	94.96
FS-LSTM	92.95	93.78	94.10	98.14
XSRU-IoMT	98.39	96.89	91.75	96.88
ESHCS-DLJSO	99.43	99.14	99.14	99.14

Table 4. Comparative analysis of ESHCS-DLJSO technique with recent methods[48–50].

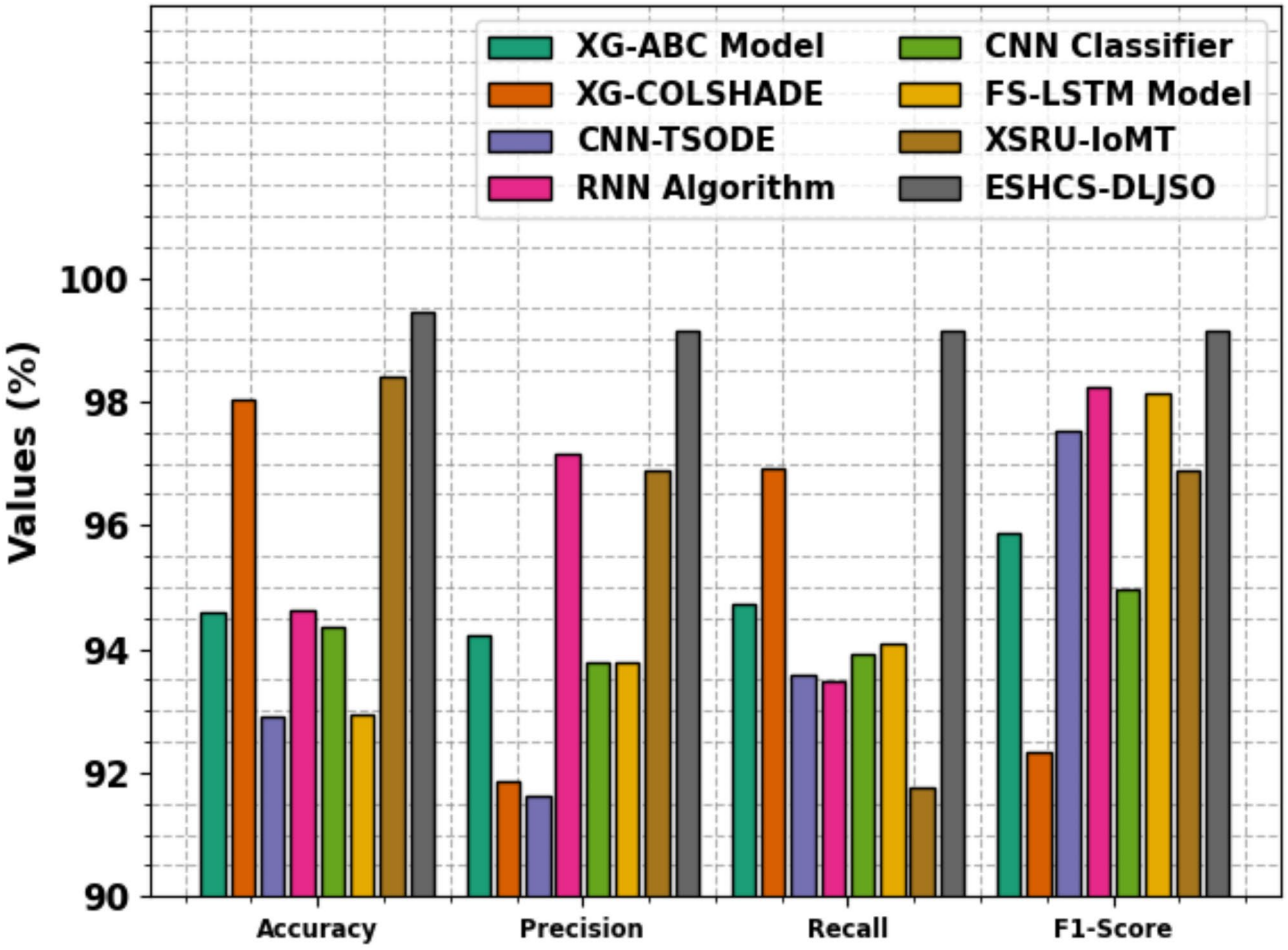

Fig. 13. Comparative analysis of ESHCS-DLJSO technique with recent methods.

Method	CT (s)
XG-ABC	5.98
XG-COLSHADE	8.98
CNN-TSODE	11.21
RNN	8.64
CNN Classifier	13.33
FS-LSTM	5.88
XSRU-IoMT	10.79
ESHCS-DLJSO	3.89

Table 5. CT analysis of ESHCS-DLJSO technique with recent methods.

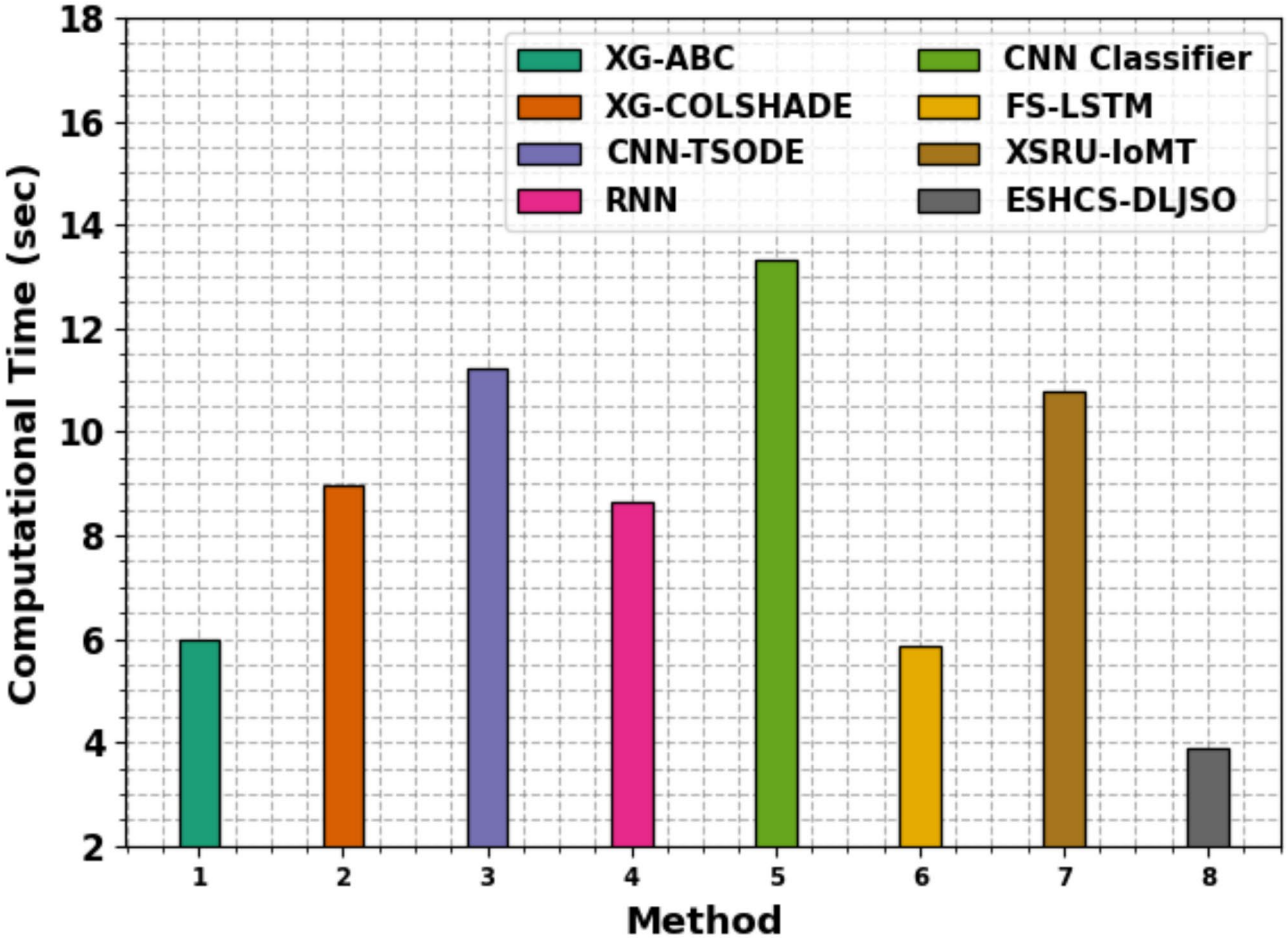

Fig. 14. CT analysis of ESHCS-DLJSO technique with recent methods.

Data availability

The datasets used and analyzed during the current study available from the corresponding author on reasonable request.

Received: 12 August 2024; Accepted: 2 April 2025
Published online: 17 April 2025

References

1. Ksibi, A. et al. Secure and fast emergency road healthcare service based on blockchain technology for smart cities. *Sustainability*. **15**(7), 5748 (2023).
2. Hathaliya, J. J. & Tanwar, S. An exhaustive survey on security and privacy issues in healthcare 4.0. *Comput. Commun.* **153**, 311–335 (2020).
3. Krishnamoorthy, S., Dua, A. & Gupta, S. Role of emerging technologies in future IoT-driven healthcare 4.0 technologies: A survey, current challenges and future directions. *J. Ambient Intell. Humaniz. Comput.* **14** (1), 361–407 (2023).
4. Alnaim, A. K. & Alwakeel, A. M. Machine-learning-based IoT–edge computing healthcare solutions. *Electronics*. **12**(4), 1027 (2023).
5. Ali, O. et al. A systematic literature review of artificial intelligence in the healthcare sector: Benefits, challenges, methodologies, and functionalities. *J. Innov. Knowl.* **8**(1), 100333 (2023).
6. Ali, M. H. et al. Threat analysis and distributed denial of service (DDoS) attack recognition in the internet of things (IoT). *Electronics*. **11**(3), 494 (2022).
7. Mohammed, K. I. et al. Real-time remote-health monitoring systems: a review on patients prioritisation for multiple-chronic diseases, taxonomy analysis, concerns and solution procedure. *J. Med. Syst.* **43**, 1–21 (2019).
8. Zaher, M. A. & Nabil, M. E. Intelligent data fusion model for electrocardiogram classification for efficient decision making in the healthcare sector. *Fusion Pract. Appl.* **9** (1), 47–58 (2022).
9. Valsalan, P., Baomar, T. A. B. & Baabood, A. H. O. IoT based health monitoring system. *J. Crit. Rev.* **7** (4), 739–743 (2020).
10. Durán-Vega, L. A. et al. An IoT system for remote health monitoring in elderly adults through a wearable device and mobile application. *Geriatrics*. **4**(2), 34 (2019).
11. Mohapatra, A. D., Aggarwal, A. & Tripathy, R. K. Automated rec gnition of hand gestures from multichannel EMG sensor data using time-frequency domain deep learning for IoT applications. *IEEE Sens. Lett.* (2024).
12. Wang, Z., Li, F., Xu, J. & Cosman, P. C. Human–machine interaction-oriented image coding for resource-constrained visual monitoring in IoT. *IEEE Internet Things J.* **9** (17), 16181–16195 (2022).

13. Islam, M. R. et al. Deep learning-based IoT system for remote monitoring and early detection of health issues in real-time. *Sensors*. **23**(1), 5204 (2023).
14. Rani, S., Jining, D., Shoukat, K., Shoukat, M. U. & Nawaz, S. A. A human–machine interaction mechanism: Additive manufacturing for industry 5.0—design and management. *Sustainability*. **16**(10), 4158 (2024).
15. Mao, J. et al. A health monitoring system based on flexible triboelectric sensors for intelligence medical internet of things and its applications in virtual reality. *Nano Energy*. **18**, 108984 (2023).
16. Webber, J., Mehbodniya, A., Teng, R. & Arafa, A. Human–Machine interaction using probabilistic neural network for light communication systems. *Electronics*. **1**(6), 932 (2022).
17. Shoukat, M. U. et al. Smart home Fo enhanced healthcare: exploring human machine interface oriented digital twin model. *Multimed. Ls Appl.* **83** (11), 31297–31315 (2024).
18. Nguyen, H. Q. et al. Hand gesture recognition from wrist-worn camera for human–machine interaction. *IEEE Access*. **1**, 53262–53274 (2023).
19. Vakili, A. et al. A new service composition method in the cloud-based internet of things environment using a grey Wolf optimization algorithm and mapreduce framework. *Concurr. D Comput. Pract. Exp*. **36** (16), e8091 (2024).
20. Heidari, A., Navimipour, N. J., Dag, H., Talebi, S. & Unal, M. A novel blockchain-based deepfake detection method using federated and deep learning models. *Cogn. Comput.*, 1–19 (2024).
21. Pavithra, D., Nidhya, R., Shanthi, S. & Priya, P. A secured and optimized deep recurrent neural network (DRNN) scheme for remote health monitoring system with edge computing. *Automatika: časopis za automatiku, mjerenje, elektroniku, računarstvo i komunikacije*. **64**(3), 508–517 (2023).
22. Aminizadeh, S. et al. Opportunities and challenges of artificial intelligence and distributed systems to improve the quality of healthcare service. *Artif. Intell. Med.* **149**, 102779 (2024).
23. Amiri, Z., Heidari, A., Navimipour, N. J., Esmaeilpour, M. & Yazdani, Y. The deep learning applications in IoT-based bio-and medical informatics: a systematic literature review. *Neural Comput. Appl.* **36** (11), 5757–5797 (2024).
24. Kumar, P. et al. A blockchain- Rchestrated deep learning approach for secure data transmission in IoT-enabled healthcare system. *J. Parallel Distrib. Comput.* **172**, 69–83 (2023).
25. Heidari, A., Shishehlou, H., Darbandi, M., Navimipour, N. J. & Yalcin, S. A reliable method for data aggregation on the industrial internet of things using a hybrid optimization algorithm and density correlation degree. *Cluster Comput.*, 1–19 (2024).
26. Heidari, A., Navimipour, N. J. & Unal, M. A secure intrusion detection platform using blockchain and radial basis function neural networks for internet of drones. *IEEE Internet Things J.* **10** (10), 8445–8454 (2023).
27. Heidari, A., Amiri, Z., Jamali, M. A. J. & Jafari, N. Assessment of reliability and availability of wireless sensor networks in industrial applications by considering permanent faults. *Concurr. Comput. Pract. Exp.*, e8252 (2024).
28. Singh, N. P. et al. August. Enhancing Hea thcare Security Using IoT-Enabled with Continuous Authentication Using Deep Learning. In *International Conference on Electrical and Electronics Engineering* 275–289 (Springer Nature Singapore, 2023).
29. Zanbouri, K. et al. A GSO-based multi-objective technique for performance optimization of blockchain-based industrial internet of things. *Int. J. Commun. Syst.* **37** (15), e5886 (2024).
30. Amiri, Z., Heidari, A. & Navimipour, N. J. Comprehensive survey of artificial intelligence techniques and strategies for climate change mitigation. *Energy*. 13227 (2024).
31. Rajkumar, G., Devi, T. G. & Srinivasan, A. Heart disease prediction using IoT based framework and improved deep learning approach: medical application. *Med. Eng. Phys.* **111**, 103937 (2023).
32. Aldaej, A., Ahanger, T. A. & Ullah, I. Deep neural network-based secure healthcare framework. *Neural Comput. Appl.*, 1–16 (2024).
33. Movassagh, A. A. et al. Artificial neural networks training algorithm integrating invasive weed optimization with differential evolutionary model. *J. Ambient Intell. Humaniz. Comput.*, 1–9 (2023).
34. Babar, M. et al. An efficient and hybrid deep learning-driven model to enhance security and performance of healthcare internet of things. *IEEE Access.* (2025).
35. Kumar, K. S. et al. A secure and efficient BlockChain and distributed Ledger technology-based optimal resource management in digital twin beyond 5G networks using hybrid energy valley and levy Flight Distributer Optimization algorithm. *IEEE Access*. (2024).
36. Othmen, S. et al. Enhancing IoT-enabled healthcare applications by efficient cluster head and path selection using fuzzy logic and enhanced particle swarm optimization. *Int. J. Commun. Syst.* **38** (3), 6096 (2025).
37. Alzubi, J. A. Blockchain-based Lamport Merkle digital signature: authentication tool in IoT healthcare. *Comput. Commun.* **170**, 200–208 (2021).
38. Rani, V. V., Vasavi, G., Paul, P. M. & Rani, K. S. IoT based healthcare system using fractional dung beetle optimization enabled deep learning for breast cancer classification. *Comput. Biol. Chem.* **114**, 108277 (2025).
39. Alzubi, J. A., Alzubi, O. A., Singh, A. & Ramachandran, M. Cloud-IIoT-based electronic health record privacy-preserving by CNN and blockchain-enabled federated learning. *IEEE Trans. Ind. Inf.* **19** (1), 1080–1087 (2022).
40. Radhika, B., Fathima, N., Leelavathi, V. V. & Pratibha, S. BBOA-SNDAE: A deep learning model for HD prediction in medical IoT systems. *J. Intell. Syst. Internet Things*. **14**(1). (2025).
41. Naz, A., Khan, H., Din, I. U., Ali, A. & Husain, M. An efficient optimization system for early breast cancer diagnosis based on internet of medical things and deep learning. *Eng. Technol. Appl. Sci. Res.* **14** (4), 15957–15962 (2024).
42. Bai, Y., Gu, B. & Tang, C. Enhancing real-time patient monitoring in intensive care units with deep learning and the internet of things. *Big Data*. (2025).
43. Henderi, H., Wahyuningsih, T. & Rahwanto, E. Comparison of Min-Max normalization and Z-Score normalization in the K-nearest neighbor (kNN) algorithm to test the accuracy of types of breast cancer. *Int. J. Inf. Inform. Syst.* **4** (1), 13–20 (2021).
44. Zaini, F. A., Sulaima, M. F., Razak, I.A.B.W.A., Othman, M. L. & Mokhlis, H. A hybrid model based on LSSVM and the improved BFOA for sustainability of daily electricity load forecasting in Malaysia (2024).
45. Fan, Y., Ma, Z., Tang, W., Liang, J. & Xu, P. Using crested Porcupine optimizer algorithm and CNN-LSTM-Attention model combined with deep learning methods to enhance short-term power forecasting in PV generation. *Energies*. **17**(4), (2024).
46. Abd-El Wahab, A. M., Kamel, S., Hassan, M. H., Sultan, H. M. & Molu, R. J. J. *An Effective Gradient Jellyfish Search Algorithm for Optimal Reactive Power Dispatch in Electrical Networks* (IET Generation, Transmission & Distribution, 2024).
47. https://www.kaggle.com/datasets/faisalmalik/iot-healthcare-security-dataset.
48. Savanović, N. et al. Intrusion detection in healthcare 4.0 internet of things systems via metaheuristics optimized machine learning. *Sustainability*. *15*(16), 12563 (2023).
49. Ashraf, E., Areed, N. F., Salem, H., Abdelhay, E. H. & Farouk, A. Fidchain: fed rated intrusion detection system for blockchain-enabled Iot healthcare applications. In *Healthcare*, vol. 10, No. 6, 1110. (MDPI, 2022).
50. Alalhareth, M. & Hong, S. C. An adaptive intrusion detection system in the internet of medical things using fuzzy-based learning. *Sensors*. **23**(2), 9247 (2023).

Author contributions

Conceptualization: F.K. and M.R. Data curation and formal analysis: F.A., M.R., F.K. and O.A.A. Investigation and methodology: M.R., S.S.B., L.A.M., M.K.A.-H. Project administration and resources: M.R. Validation and visualization: S.S.B., L.A.M., O.A.A. Writing—original draft, M.R., F.K., F.A. and M.K.A.-H.Writing—review

and editing: S.S.B. and O.A.A.L.A.M . Supervision: M.K.A.-H. All authors have read and agreed to the published version of the manuscript.

Funding
This project was funded by the Deanship of Scientific Research (DSR) at King Abdulaziz University (KAU), Jeddah, Saudi Arabia, under grant no. (GPIP:300-611-2024). The authors, therefore, acknowledge with thanks DSR at KAU for technical and financial support.

Declarations

Competing interests
The authors declare no competing interests.

Ethics approval
This article contains no studies with human participants performed by any authors.

Additional information
Correspondence and requests for materials should be addressed to M.R.

Reprints and permissions information is available at www.nature.com/reprints.

Publisher's note Springer Nature remains neutral with regard to jurisdictional claims in published maps and institutional affiliations.